Journal of Hazardous Materials 452 (2023) 131181

Contents lists available at ScienceDirect

Journal of Hazardous Materials

journal homepage: www.elsevier.com/locate/jhazmat

Drought-free future climate conditions enhance cadmium phytoremediation capacity by *Brassica napus* through improved physiological status

Austra Dikšaitytė [a,*], Inesa Kniuipytė [b], Jūratė Žaltauskaitė [a]

[a] *Department of Environmental Sciences, Vytautas Magnus University, Universiteto st. 10, LT-53361 Akademija, Kaunas distr., Lithuania*
[b] *Lithuanian Energy Institute, Laboratory of Heat–Equipment Research and Testing, Breslaujos st. 3, LT-44403, Kaunas, Lithuania*

HIGHLIGHTS

- *B. napus* exhibited good tolerance to soil Cd up to 50 mg kg^{-1}.
- Shoots' nutrients correlated well with electron transport (ET)-related parameters.
- Cd-disrupted ET from OEC, PSII RCs, FNR, and PC lowered P_r more in CC conditions.
- Higher P_r and shoot DW resulted in higher Cd accumulation under FC conditions.
- FC risen the soil Cd removal rate of well-watered plants.

GRAPHICAL ABSTRACT

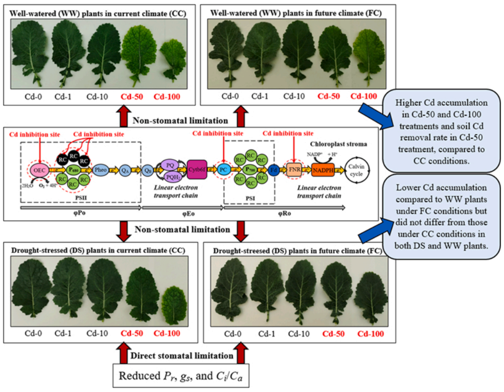

ARTICLE INFO

Editor: Guilla ume Echevarria

Keywords:
Cadmium
Brassica napus
Phytoremediation
Future climate
Drought

ABSTRACT

This study aimed to assess Cd phytoextraction efficiency in well-watered and drought-stressed *B. napus* plants under current climate (CC, 21/14 °C, 400 ppm CO_2) and future climate (FC, 25/18 °C, 800 ppm CO_2) conditions. The underlying physiological mechanisms underpinning the obtained results were investigated by studying Cd (1, 10, 50, and 100 mg kg^{-1}) effect on *B. napus* photosynthetic performance and nutritional status. Only the Cd-50 and Cd-100 treatments caused visible leaf lesions, growth retardation, reductions in both gas exchange and chlorophyll fluorescence-related parameters, and disturbed mineral nutrient balance. Under CC conditions, well-watered plants were affected more than under FC conditions. The most important pathway by which Cd affected *B. napus* photosynthetic efficiency in well-watered plants was the damage to both photosystems, lowering photosynthetic electron transport. Meanwhile, non-stomatal and stomatal limitations were responsible for the higher reduction in the photosynthetic rate (P_r) of drought-stressed compared to well-watered plants. The significantly higher shoot dry weight, which had a strong positive relationship with P_r, was the main factor determining significantly higher shoot Cd accumulation in high Cd treatments in well-watered plants under FC conditions, resulting in a 65% ($p < 0.05$) higher soil Cd removal rate in the Cd-50 treatment.

---

* Corresponding author.
E-mail address: austra.diksaityte@vdu.lt (A. Dikšaitytė).

https://doi.org/10.1016/j.jhazmat.2023.131181
Received 29 September 2022; Received in revised form 13 February 2023; Accepted 7 March 2023

1. Introduction

A steady rise in atmospheric carbon dioxide (CO_2) concentration, which, according to the Global Monitoring Laboratory (GML) of the National Oceanic and Atmospheric Administration (NOAA), in 2021, reached the average level of 415 ppm, setting a new record high despite the ongoing economic drag from the COVID-19 pandemic [56]. The constant rise of greenhouse gases (GSH), in particular CO_2 emissions, has caused a dangerous rise in global land surface temperature, known as global warming, which in turn has resulted in an alarming increase in the frequency and intensity of abiotic stresses, such as extended drought periods [73]. According to the latest Intergovernmental Panel on Climate Change (ICCP) report, global surface temperature will continue to rise until at least the mid-century, adding 3.6 °C, on average, by 2100 compared to 1850–1900 under the Shared Socioeconomic Pathways (SSPs) regional rivalry scenario (SSP 3–7.0) with high GHG and CO_2 emissions. However, not all regions will be equally affected. Europe is warming faster than the global average. Temperatures in Europe rise more than twice the global average at a rate of about + 0.5 °C per decade from 1991 to 2021 [84]. According to Coupled Model Intercomparison Project Phase 6 (CMIP6) projections, temperatures across European land areas will continue to rise faster than the global average throughout the century [29]. Meanwhile, continued global warming is projected further intensify the severity of extreme climatic events, such as drought [39].

Another global issue of growing importance is increasing soil contamination by cadmium (Cd) [106,33,79]. As urbanization, industrialization, and intensive agriculture are expanding [90,101], large amount of Cd is constantly added to the soil-plant-environment system [3,79]. Unlike essential heavy metals (HM), such as Cu, Fe, Mn, Zn, etc., that are either nontoxic or significantly less harmful at low concentrations, non-essential metals like Cd, Hg, and Pb, are highly hazardous to all living organisms at even low concentrations [46,45]. In addition, compared to the other HM, Cd has the highest water solubility [38] and thus is one of the most mobile elements in the environment [49] with a severe extent of bioaccumulation [106]. Contrary to lead and mercury ions, plants readily absorb cadmium ions [79], allowing Cd to be easily transferred into the food chain via contaminated agricultural products and accumulate in the human body, posing a significant risk to human health [32,94]. Consequently, Cd is regarded as one of the most hazardous materials [3,45]. Cd critical risk thresholds in soil vary by country, ranging from 0.4 $mg\ kg^{-1}$ for agricultural soils to 1400 $mg\ kg^{-1}$ for industrial land use at the European level [6]. However, the mean Cd value in the arable soils far exceeds the limits for agricultural soils in different regions (e.g., [2,24,58,100]). As a result, natural and agricultural ecosystems are experiencing both pollution-related and climate-related stresses, with climate-related stress becoming more frequent and intense with each additional increment of global temperature [39].

Although conventional remediation technologies can be used to immobilize, remove, or detoxify HM in soil, these approaches-associated environmental, social, and economic impacts confine their overall sustainability [70,96]. Therefore, there is a need to transition from conventional to eco-safe, nature-based solutions, saving energy through the emergence and development of green and sustainable remediation technologies such as phytoremediation, a promising plant-based approach for the cost-effective revegetation of HM-contaminated soil [4,101]. Among phytoremediation techniques, the most attention has received phytoextraction, which employs plants for the extraction of HM from soils and their accumulation in harvestable biomass, ensuring a permanent solution for the removal of HM from polluted soil [101,11,90]. Plant performance and consequently efficiency of phytoextraction is highly dependent on climate conditions, therefore it may be restricted or accelerated by changing climate conditions. Given ongoing climate change, good adaptation to the prevailing environment may become one of the main plant features, determining its phytoextraction potential.

Climate conditions such as elevated CO_2, warming, and drought may significantly influence plants growing in heavy-metal polluted soil, either positively or negatively [71]. Elevated CO_2 showed the potential to improve the phytoremediation of Cd-contaminated soils by increasing aboveground plant biomass or Cd concentration in the aboveground part [55,105]. Warming also tended to increase Cd accumulation in the aboveground parts of different plant species, but the effect varied depending on species and genotype (e.g., [27,69]). Meanwhile, Cd uptake and plant accumulation under drought conditions vary with species and cultivars, plant developmental stages, and duration of the water stress, with both increases and decreases being reported [1,57,81,98]. However, mechanisms involved in Cd accumulation under changing climate conditions are so far less studied, and the simultaneous presence of Cd in growth media, combined with all these soil and climate change-related variables, has not yet been investigated, to our knowledge.

Well-watered and drought-stressed pot-grown rapeseed (*Brassica napus*), as a multipurpose fast-growing annual crop with high biomass production, was used in the current research to investigate its potential for Cd phytoextraction purposes in the current and future climate conditions with elevated temperature and CO_2. Rapeseed, one of the major oilseed crops worldwide and a promising biofuel crop [97], combined with phytoextraction can significantly contribute to the economy. Besides, *B. napus* photosynthetic rate and above-ground biomass production were shown to increase considerably under high air temperature conditions, especially in conjunction with elevated CO_2, while drought only marginally retarded their growth [12,13,43], implying the higher possible potential for phytoextraction under future climate conditions. Therefore, the objectives of this study were to (1) assess Cd accumulation efficiency in well-watered and drought-stressed repressed plants grown under current climate and future climate conditions in determining the best conditions for phytoextraction and (2) explore some of the underlying physiological mechanisms underpinning the obtained results by studying Cd effect on rapeseed photosynthetic performance and nutritional status.

2. Materials and methods

2.1. Characterization of experimental soil and plant material

The experimental soil (Calcari-Endohypogleyic Luvisol) was collected from the surface layer (0–20 cm) of the field soil in the Academy of Agriculture Experimental Research Station of Vytautas Magnus University in Kaunas district, Lithuania. The collected soil was crushed into particles up to 10 × 10 mm in size and thoroughly mixed with agroperlite and sand (fraction 0–2 mm) in a 5:3:2 vol ratio for the pot experiment. For soil characteristics analysis, part of the prepared soil sample was air-dried and passed through a 2-mm sieve. The main physical and chemical characteristics of the mixed soil were as follows: soil pH (1 $mol\ L^{-1}$ KCl, ISO 10390) of 6.7 ± 0.1, electrical conductivity (ISO 11265) of 6.6 ± 0.08 $mS\ m^{-1}$, organic carbon (ISO 10694), humus (ISO 10694), and organic matter (ISO 10694) of 8.1 ± 0.1 $g\ kg^{-1}$, 14 ± 0.2 $g\ kg^{-1}$ and 19 ± 0.1 $g\ kg^{-1}$, respectively, mineral nitrogen ($N\text{-}NO_3$ + $N\text{-}NO_2$ and $N\text{-}NH_4$, ISO 13395 and ISO 11732, respectively) of 22 ± 0.3 $mg\ kg^{-1}$, available phosphorus and potassium, determined by Egner-Riehm-Domingo (A-L) method [19], of 121 ± 4.5 $mg\ kg^{-1}$ and 68 ± 1.0 $mg\ kg^{-1}$, respectively, and available sulfur, calcium, and magnesium, determined according to LVP D-12:2021 and LVP D-13:2021 standards, of 2.7 ± 0.1 $mg\ kg^{-1}$, 1588 ± 26.5 $mg\ kg^{-1}$ and 269 ± 4.5 $mg\ kg^{-1}$, respectively.

The rapeseed seeds (var. 'Fenja') were provided by the Institute of Agriculture of the Lithuanian Research Centre for Agriculture and Forestry.

2.2. Design of cadmium remediation experiment

The pot experiment was conducted in 10 m^3 growth chambers (2.0 ×

2.0 × 2.5 m width, length, and height) with the controlled environment operating cupboards (Emerson Network Power S.r.l., Italy, model No. S06UC021V300020FX051260) under a completely randomized design using three factors: (i) cadmium, (ii) climate conditions, and (iii) soil moisture level. The prepared soil was spiked with a heavy metal solution applied as $CdCl_2 \times 2.5\ H_2O$ and mixed thoroughly to prepare the artificial Cd-contaminated soil with five Cd concentrations: 0 (control, no amended with cadmium), 1, 10, 50, and 100 mg kg^{-1}. Then a total of 2.5 kg of processed soil was placed into each plastic pot (a 21-cm top diameter, a 15-cm bottom diameter, a 10.6-cm height, and a 3-L capacity) and mixed well with NPK (12–11–18 + microelements) compound fertilizer (Achema, Lithuania) at a rate of 60 kg N ha^{-1} for basal fertilization.

Pots were randomly divided into two groups, one of which was placed in the growth chamber with preset current climate (CC) conditions (ambient CO_2 set at 400 ppm, 14/10 h ambient air temperature set at 21/14 °C, and 14/10 h of 55–60/65–70% relative humidity (RH)) and another one was placed in the growth chamber with preset future climate (FC) conditions (elevated CO_2 set at 800 ppm, 14/10 h elevated air temperature set at 25/18 °C, and 14/10 h of 45–50/55–60% RH). The ambient air temperature was defined according to the long-term average temperature of the vegetation period in Lithuania. The elevated air temperature and CO_2 concentration were selected according to the predictions of the latest ICCP report based on the SSP3–7.0 scenario with high GHG and CO_2 emissions, which will roughly double from current levels by 2100 [39]. According to the SSP3–7.0 scenario and regional models, Europe's projected land temperature rise at the end of the century (2081–2100) will reach + 4 °C [92]. Other growing conditions like photoperiod and photosynthetically active radiation (PAR) were maintained identically in both chambers as follows: 14/10 h light/dark regime and ~ 300 mol m^{-2} s^{-1} PAR at the leaf level delivered by a combination of natural daylight luminescent lamps (Philips, Waterproof OPK Natural Daylight LF80 Wattage 2 × 58 W/TL-D 58 W) and high-pressure sodium lamp (Philips MASTER GreenPower CG T 600 W). Temperatures in the growth chambers were manually adjusted in the operating cupboards, whereas CO_2 concentration was automatically adjusted by adjusting the amount of injected CO_2 gas and the chamber conditioner. An Interactive Graphical SCADA System (IGSS) software (version 9–13175) was used to control the climate program. The CO_2, temperature, and humidity transmitter with display (CO2HRT-D, Regin, Källered, Sweden) was used to record the climate parameters inside the growth chambers.

Randomly arranged pots with three replicates per Cd-treatment were left for stabilization in the chambers under simulated CC and FC conditions for seven days. After this, rapeseed seeds were directly sowed into these pots (15 units per pot), and then they were thinned to seven plants per pot after three weeks of sowing. To avoid nutrient deficiency, on the 34th day after sowing (DAS), plants were additionally fertilized with the NPK compound fertilizer at a rate of 60 kg N ha^{-1}. A constant level of 30% of volumetric soil water content (SWC), measured at a depth of 6 cm using a ThetaProbe ML2x type soil moisture sensor and HH2 type moisture meter (Delta-T Devices Ltd., Cambridge, UK), was maintained in both chambers during this period using tap water.

On the 46th DAS, half of the pots in each chamber were randomly selected for drought treatment, and drought stress (designated as DS) was started by withholding watering until the SWC dropped to an average of 5%. Then, DS-treated plants were kept at the SWC of 5% until the end of the experiment, totaling 12 days of drought stress at this soil moisture level. Meanwhile, the SWC of 30% was continuously maintained for well-watered plants (designated as WW). Overall, twenty treatments, replicated three times, were set up, resulting in a total of 60 pots, i.e. 5 Cd concentrations (Cd-0, Cd-1, Cd-10, Cd-50, and Cd-100) × 2 climate conditions (CC and FC) × 2 soil moisture levels (WW and DS) × 3 replicates.

To avoid the effect of the chamber on plant growth, the growth chambers were used in randomized order, moving the pots from one chamber to another twice during the experiment with restored the required climatic conditions. Pots in the same chamber were rotated every other day to avoid an "edge" effect. Plants were harvested at 64 DAS.

2.3. Plant sample collection and analysis

After being harvested, plants were separated into shoots and roots. Roots were washed thoroughly with tap water to remove all potting materials, rinsed with deionized water, and drained with a paper towel before weighing. Then fresh biomass of the separated shoots and roots was recorded, after which plant samples were dried at 70 °C in a forced-air ventilation oven (Venticell LSIK-B2V/VC 111, Germany) to a constant dry weight (DW) and weighed again with a balance (Kern ADB 200–4, Germany). The shoots and roots DW of seven samples per pot were calculated into DW per plant and averaged as the values of three biological replicates.

Dried root and shoot samples were pulverized, powdered with a mill (Retsch MM400, Germany), and stored in air-tight bags at room temperature until analysis. To determine the rapeseed Cd and nutrient concentrations, the milled shoots and roots samples (~ 0.2 g) were digested with 65% HNO_3 and 30% H_2O_2 solutions (v/v = 8/2) using a microwave digester (Milestone ETHOS One, Italy). The Cd, P, K, Ca, Mg, S, Fe, Mn, Cu, and Zn concentrations in digested shoots and roots extracts were analyzed by inductively coupled plasma optical emission spectrometry (ICP-OES) on an Optima 8000 (PerkinElmer, USA). Certified reference materials (CRMs) approved by the Community Bureau of Reference (BCR), CRM − BCR − 129 Hay Powder and CRM – BCR − 482 Lichen (Institute for Reference Materials and Measurements), as well as blank reagent samples, were used to ensure the accuracy of the analytical methods. The calibration standards were analyzed every 20 samples to monitor the ICP-OES signal drift. Each of the samples has been scanned a total of three times.

2.4. Phytoremediation efficiency

Cd accumulation in shoots and roots, bioconcentration factor (BCF), and soil Cd removal rate [10,53] were used to evaluate rapeseed phytoextraction efficiency under CC and FC conditions at different soil moisture levels (WW and DS). The following equations were used to compute these evaluations:

$$\mathrm{Cd_{accu}} - \mathrm{SorCd_{accu}} - \mathrm{R} = \mathrm{Cd_{shoot}} \times \text{shoot DW or } \mathrm{Cd_{root}} \times \text{ root DW} \tag{1}$$

$$\mathrm{BCF} = \frac{\mathrm{Cd_{shoot}}}{\mathrm{Cd_{soil}}} \tag{2}$$

$$\text{Cd removal rate } (\%) = \frac{\mathrm{Cd_{accu}} - \text{Sper pot}}{\mathrm{Cd_{soil}} \times \mathrm{Weight_{soil}}} \times 100\% \tag{3}$$

where Cd_{accu}-S and Cd_{accu}-R are Cd accumulation (mg) in shoots and roots, respectively; Cd_{shoot} and Cd_{root} are Cd concentration (mg kg^{-1} DW) in shoots and roots, respectively; Cd_{soil} is Cd concentration (mg kg^{-1}) in soil; shoot DW and root DW are shoot and root dry weight (mg), respectively; and $Weight_{soil}$ is the soil weight (kg) in the pot. The shoot dry weight, Cd concentration, and accumulation in shoots were calculated on a one-plant basis per pot. Each pot contained seven plants.

2.5. Photosynthetic efficiency

Photosynthetic efficiency, estimated by leaf gas exchange and chlorophyll fluorescence-related parameters, was determined on 63 DAS with the youngest fully expanded leaves using a portable infrared leaf gas exchange system LI-6400 (LI-COR Inc., NE, USA) and a Plant Efficiency Analyzer Handy PEA (Hansatech Instruments, King's Lynn, Norfolk, England), respectively.

For gas exchange, the measurements of nine biological replicates per variant (three pots with three randomly selected plants each) were recorded, taken under the same leaf chamber conditions as the plants were growing in the growth chambers. The block temperature and CO_2 concentration of the reference cell were set at 21 °C and 400 μmol mol^{-1} or 25 °C and 800 μmol mol^{-1} to reflect CC and FC conditions, respectively. The RH inside the leaf cuvette was allowed to vary with growth chamber conditions. The airflow rate through the assimilation chamber was maintained at 500 μmol s^{-1} for all gas exchange measurements, and PAR outside the leaf cuvette between all the treatments in the CC and FC chambers averaged 207 ± 1.4 and 211 ± 2.0 μmol m^{-2} s^{-1} ($p > 0.05$), respectively. The C_i/C_a ratio was calculated by dividing the intercellular CO_2 concentration (C_i) by ambient CO_2 concentration (C_a, 400 or 800 μmol mol^{-1}), and the water use efficiency (WUE, μmol CO_2 $mmol^{-1}$ H_2O) was calculated as the ratio of photosynthetic rate (P_r) and transpiration (E).

The chlorophyll *a* fluorescence was measured on the middle section of the leaves' upper side. Before the measurements, leaves were adapted to darkness for 15 min. Then the dark-adapted leaves were exposed to a 1-s saturating ultra-bright red-light pulse (650 nm) with an intensity of 1800 μmol photons m^{-2} s^{-1} flashed by an array of three light-emitting diodes with uniform irradiation on the leaf surface exposed by the leaf clip with a diameter of 4 mm. Chlorophyll *a* fluorescence data were processed with WINPPEA software version 32, provided with the Plant Efficiency Analyser. The biophysical parameters were derived from the O-J-I-P transients, where O stands for origin (the minimum fluorescence, Fo, recorded at the intensity of 50 s) when all reaction centers (RCs) of photosystem II (PSII) are assumed to be open, J and I for two intermediate levels at 2 ms and 30 ms (FJ and FI), and P for peak (FP or FM), the maximal intensity when all PSII RCs are closed, which is usually in the ~ 500-ms range [87]. The measured data were used for the calculation according to the JIP-test equations. The following parameters, which refer to the time of maximal intensity, were used: (i) Flux ratios of PSII: φPo, ψEo, and φEo (ii) flux ratios of PSI: δRo and φRo (iii) Performance indexes on an absorption basis (combination of parameters expressing partial potentials at steps of energy bifurcations of PSII and specific electron transport reactions): PIabs, PItotal, and SFIabs. The formulas, definitions, and references of JIP-test parameters are presented in Table 1.

Table 1

The formulas and definitions of JIP-test parameters, derived using data extracted from the fast fluorescence transient O-J-I-P. PSI, PSII, RC, Q_A, and PQ stand for photosystem I, photosystem II, active PSII reaction centers, the first plastoquinone electron acceptor of PSII, and plastoquinone, respectively.

Parameters	Formulas	Definitions	References [a]
Quantum yields and efficiencies/probabilities			
φPo	= Fv/Fm = TRo/ABS = 1 − Fo/Fm	Maximum quantum yield of primary photochemistry reactions in PSII RC	1 − 8
ψEo	= ETo/TRo = 1 − V_J	Efficiency/probability that PSII trapped electron moves future than Q_A^- (i.e. is transferred from Q_A^- to PQ)	1 − 8
φEo	= ETo/ABS = φPo × ψEo	Quantum yield of electron transport (ET) from Q_A^- to PQ	1 − 5, 7, 8
δRo	= REo/ETo = (1 − V_I)/ψEo	Efficiency/probability with which an electron from the intersystem electron carriers is transferred to reduce end electron acceptors at the PSI acceptor side	2 − 5, 8
φRo	= REo/ABS = φPo × (1 − V_I)	Quantum yield for reduction of end electron acceptors at the PSI acceptor side	2 − 4, 8
Performance indexes on an absorption basis			
PIabs	= (RC/ABS) × [φPo/(1 − φPo)] × [ψEo/(1 − ψEo)]	Performance index (potential) for energy conservation from photons absorbed by PSII antenna to the reduction of intersystem electron acceptors	1 − 8
PItotal	= PIabs × [δRo/(1 − δRo)]	Performance index for energy conservation from photons absorbed by PSII antenna to the reduction of PSI end acceptors	2 − 6, 8
SFIabs	= RC/ABS × φPo × ψEo	Structure-function index, which reflects changes that "favor" photosynthesis	4

[a] – 1 [88]; 2 [89]; 3 [86]; 4 [87]; 5 [44]; 6 [76]; 7 [50]; 8 [21]

2.6. Statistical analysis

The one-way analysis of variance (ANOVA) followed by Fisher's Least Significant Difference (LSD) test was used to detect any significant difference between treatments ($p < 0.05$). Three-way ANOVA was performed to determine the possible interaction between the three factors: soil Cd concentrations (0, 1, 10, 50, and 100 mg kg^{-1}), climate conditions (CC: current climate, FC: future climate), and soil moisture levels (regular soil moisture, designated as WW: well-watered, and reduced soil moisture, designated as DS: drought-stressed). Pearson's correlation analysis was conducted to determine the relationships among all the measured variables under different soil moisture and climate conditions (CC-WW, CC-DS, FC-WW, and FC-DS). Hierarchical cluster analysis (HCA) was used to create heatmaps with dendrograms using Euclidean distance as a similarity measure and group average as the clustering method. Statistical analyses were performed using STATISTICA 8, and figures were created with Microsoft Excel 2010. Origin 2020b SR0 software was used to analyze hierarchical clusters, draw heatmaps, compute Pearson correlations, and draw correlation matrixes.

3. Results

3.1. Impact of climate and soil moisture conditions on Brassica napus growth response to cadmium

Under both climatic conditions and soil moisture levels, Cd phytotoxicity symptoms on rapeseed leaves, including chlorosis, curled leaves, and stunted growth, were only seen in high Cd treatments of 50 and 100 mg Cd kg^{-1} (Cd-50 and Cd-100). However, both well-watered (WW) and drought-stressed (DS) plants grew better under future climate (FC) than current climate (CC) conditions, with fewer visible Cd toxicity symptoms (Fig. 1A-D). A three-way ANOVA performed to investigate the potential interactions between the three factors: Cd concentrations, climate conditions, and soil moisture levels showed that all three variables had a significant effect on rapeseed growth, expressed in terms of shoot and root dry weight (DW) production, but their interactions differed for shoots and roots (Table S1). Drought significantly reduced rapeseed shoot DW in Cd-0–Cd-10 treatments under CC conditions and in all Cd treatments under FC conditions by 40% on average. Root DW significantly decreased in Cd-1 and Cd-10 treatments under CC conditions by 34% on average and in Cd-1, Cd-50, and Cd-100 treatments under FC conditions by 20%, 40%, and 62%, respectively (Fig. 2 A, B). In contrast, FC conditions favored non-Cd-affected and Cd-stressed repressed growth at both soil moisture levels, alleviating the induced stress of high Cd treatments for both shoot and root DW production, except shoot DW of DS plants. Compared with the respective controls, under CC conditions, Cd-50 and Cd-100 treatments reduced shoot DW of rapeseed plants by 46% and 68% ($p < 0.05$) in the regular water regime and by 29% ($p > 0.05$) and 60% ($p < 0.05$) in the water stress regime, respectively. Meanwhile, under FC conditions, WW plants reduced shoot DW by 26% and 53%, respectively, and DS plants by 40% and 63% ($p < 0.05$) (Fig. 2 A and 5A-D). Root DW in Cd-50 and Cd-100 treatments under CC conditions decreased by 58% and 79% with regular soil moisture and 46% and 85% with drought stress conditions ($p < 0.05$), respectively. Under FC conditions, root DW of WW and DS plants decreased by 18% and 45% in the Cd-50 treatment and by 42% and 76% in the Cd-100 treatment, respectively ($p < 0.05$) (Figs. 2B and

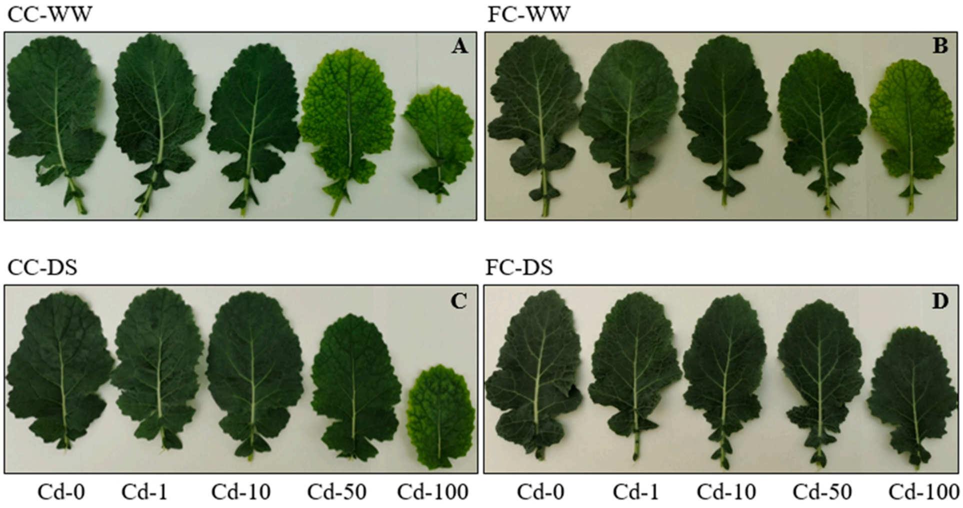

Fig. 1. Visual symptoms in leaves of rapeseed exposed to Cd treatments (Cd-0, Cd-1, Cd-10, Cd-50, and Cd-100) under well-watered (WW) conditions in the current climate (CC) and future climate (FC) (A and B, respectively) and drought-stressed (DS) conditions in CC and FC (C and D, respectively).

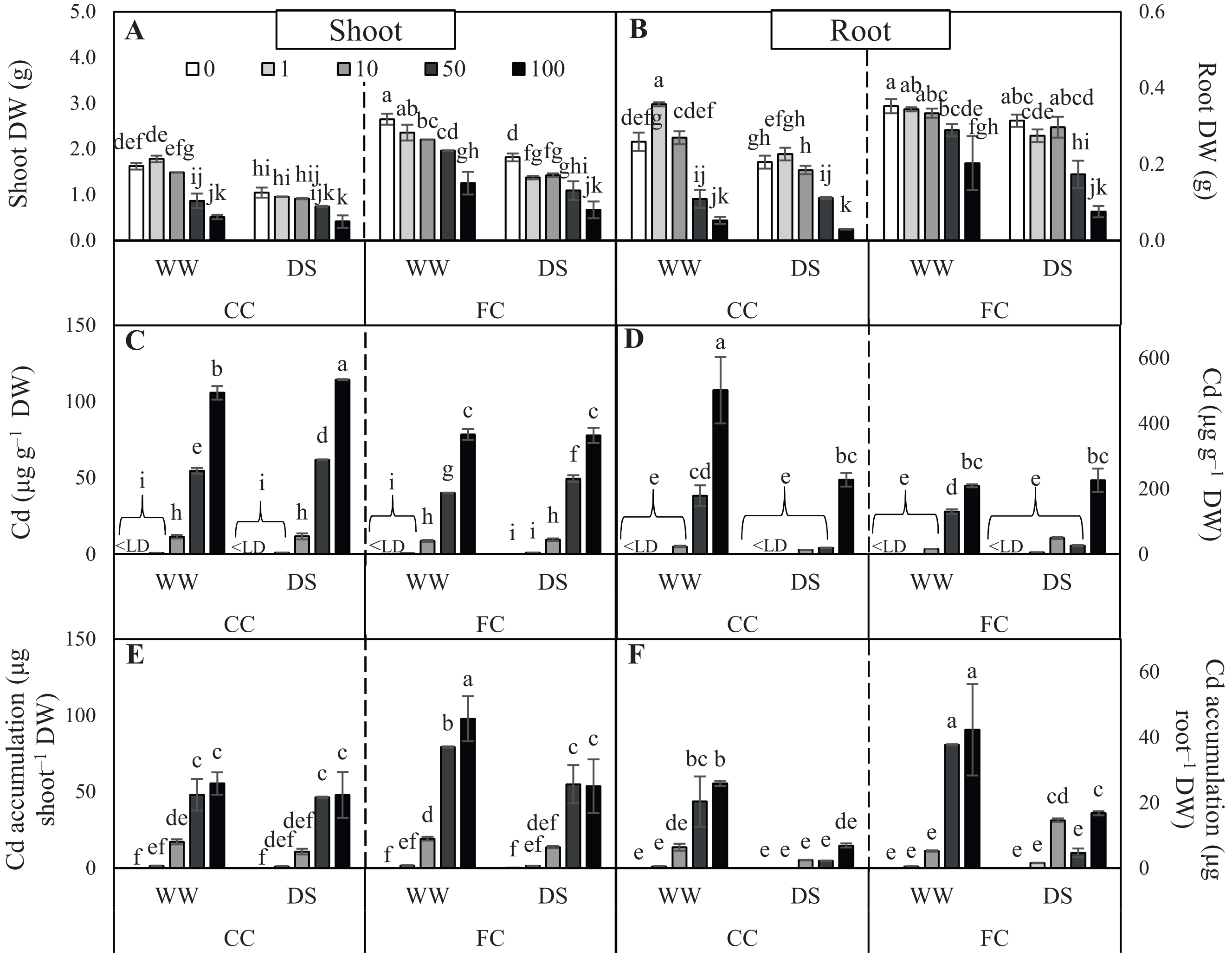

Fig. 2. Rapeseed growth and Cd concentration and accumulation under different soil Cd concentrations (0, 1, 10, 50, and 100 mg kg^{-1}), climate conditions (CC: current climate, FC: future climate), and soil moisture levels (WW: well-watered, DS: drought-stressed). A and B: Shoot and root dry weight (DW), respectively; C and D: Cd concentration in shoots and roots, respectively; E and F: Cd accumulation in shoots and roots, respectively. Data are means ± SE (n = 3). Different letters over the bars indicate significant differences among treatments ($p < 0.05$). < LD – below the detection limit.

5A-D).

3.2. *Impact of climate and soil moisture conditions on Cd accumulation in B. napus and other phytoremediation-related parameters*

As soil Cd concentration increased, so did rapeseed shoot Cd concentration. Future climate conditions have lowered Cd shoot concentrations regardless of the soil moisture level, while drought stress tended to increase Cd shoot concentration under both climate conditions (Fig. 2 C and 8A-D). Root Cd concentrations were significantly higher than shoot Cd concentrations and increased concentration-dependently in WW plants, with the Cd-100 treatment having significantly lower root Cd concentrations under FC conditions. Meanwhile, under both climates, Cd concentration in roots of DS plants did not differ significantly among Cd-1–Cd-50 treatments, while increased considerably in Cd-100 treatment, reaching 228 and 226 μg g^{-1} under CC and FC conditions, respectively (Figs. 2D and 8A-D). ANOVA results showed that all three factors and these factors combinations significantly affected root Cd concentration. Cd × soil moisture and Cd × soil moisture × climate conditions had no significant effect on shoot Cd concentration (Table S2). Shoot Cd accumulation was not significantly affected by the interaction of all three factors, while root Cd accumulation was not significantly affected by climate × soil moisture (Table S1). Shoot Cd accumulation in Cd-50 and Cd-100 treatments was significantly higher by 65% and 76%, respectively, under FC conditions in the regular water regime but not in the water stress regime (Fig. 2E). Under CC conditions, shoot Cd accumulation in high Cd treatments did not differ significantly between WW and DS plants, whereas it was lower in DS plants by 31% and 45% ($p < 0.05$) in Cd-50 and Cd-100 treatments, respectively, under FC conditions. Compared with WW plants, root Cd accumulation of DS plants was lower under both climate conditions in high Cd treatments by 60–89% ($p < 0.05$) (Fig. 2 F). FC conditions significantly increased repressed root Cd accumulation by 85% and 63%, respectively, in Cd-50 and Cd-100 treatments with regular soil moisture content, and by 5.9 and 2.4 times, respectively, in Cd-10 and Cd-100 treatments with drought stress conditions.

The bioconcentration factor (BCF) was significantly affected by climate and soil moisture conditions, while soil Cd removal rate by all three variables but not their interactions (Table S1). The BCF values of both WW and DS plants were lower under FC compared to CC conditions but mainly did not differ significantly. Meanwhile, under both CC and FC conditions, BCFs of DS plants tended to be higher than those of WW plants but also did not differ significantly, except for Cd-1 treatment under FC conditions. In most cases, BCF values did not differ between Cd treatments (Table 2). The soil Cd removal rate (%) tended to decrease concentration-dependently. In all Cd treatments, under both climate conditions, the soil Cd removal rate of DS plants was 3% up to 45% lower, as compared to WW plants, but significantly differed only in Cd-10 treatment under CC conditions. Contrarily, in all Cd treatments, the Cd removal rate of both well-watered and drought-stressed plants was 5% up to 76% higher under FC, compared to CC conditions, but significantly only in Cd-50 treatment in the regular water regime (Table 2).

Table 2
BCF and efficiency of Cd removal by rapeseed grown under different climate conditions and soil moisture levels.

Climate conditions and soil water regime	Cd_{soil}	BCF	Cd removal rate (%)
CC-WW	1	0.88 ± 0.08^{cde}	0.44 ± 0.03^{ab}
	10	1.16 ± 0.11^{ab}	0.48 ± 0.05^{a}
	50	1.09 ± 0.04^{abc}	0.27 ± 0.06^{cde}
	100	1.06 ± 0.04^{abcd}	0.16 ± 0.02^{de}
CC-DS	1	1.13 ± 0.07^{abc}	0.30 ± 0.02^{bcd}
	10	1.18 ± 0.19^{a}	0.31 ± 0.05^{bcd}
	50	1.24 ± 0.00^{a}	0.26 ± 0.00^{cde}
	100	1.14 ± 0.00^{ab}	0.13 ± 0.04^{e}
FC-WW	1	0.70 ± 0.17^{e}	0.46 ± 0.10^{a}
	10	0.87 ± 0.06^{bcde}	0.54 ± 0.04^{a}
	50	0.80 ± 0.00^{de}	0.44 ± 0.00^{ab}
	100	0.79 ± 0.04^{de}	0.27 ± 0.04^{cde}
FC-DS	1	1.13 ± 0.01^{abcd}	0.44 ± 0.01^{ab}
	10	0.97 ± 0.08^{ab}	0.39 ± 0.02^{abc}
	50	0.99 ± 0.04^{abcd}	0.31 ± 0.07^{bcd}
	100	0.78 ± 0.05^{de}	0.15 ± 0.05^{de}

Data are means ± SE (n = 3). Different column letters indicate significant differences between treatment means ($p < 0.05$). CC: current climate, FC: future climate, WW: well-watered, DS: drought- stressed.

3.3. *Impact of climate and soil moisture conditions on gas-exchange and chlorophyll fluorescence-related parameters of B. napus in response to Cd stress*

Cd, climate, soil moisture, and these factors' interactions (Table S1) differentially affected gas exchange parameters (Table S1). Only Cd and soil moisture conditions significantly affected all gas exchange parameters. P_r and C_i/C_a appeared to be the most sensitive, as they were not significantly affected only by the interaction of all three factors and Cd × soil moisture, respectively (Table S1). Under both climate and soil moisture conditions, the photosynthetic rate (P_r) of non-Cd affected and Cd-treated rapeseed followed the trend of shoot DW production (Fig. 3 A and 5A-D). Drought stress significantly reduced P_r by 32%, on average, in Cd-0–Cd-50 treatments under CC conditions, and by 42%, on average, across all Cd treatments under FC conditions. Meanwhile, when compared to CC conditions, under FC conditions, both WW and DS plants increased their P_r in all Cd treatments by 93% and 55%, on average, respectively. Compared with the respective controls, under CC conditions, Cd-50 and Cd-100 treatments reduced the P_r of well-watered plants by 40% and 67%, respectively, and by 33% and 60% in drought-stressed plants. Under FC conditions, these reductions in Cd-50 and Cd-100 treatments were 28% and 58% for WW plants and 40% and 67% for DS plants, respectively.

High Cd treatments significantly reduced the stomatal conductance (g_s) of WW and DS plants, which differed between climates only in the Cd-100 treatment. Under CC conditions, Cd-100 treatment reduced g_s of WW and DS plants by 36% and 25%, respectively, and by 29% and 57%, respectively, under FC conditions (Fig. 3B). When compared to regular soil moisture content, reduced soil moisture level reduced g_s in all Cd treatments under both climate conditions by 64% ($p < 0.05$), on average. Transpiration rate (E) mainly followed the trend of g_s (Figs. 3D and 5A-D). Under CC conditions, high Cd treatments reduced E of WW and DS plants by 21% and 16%, on average, respectively. Under FC conditions, the E of well-watered plants was reduced by 17% and 36% in Cd-50 and Cd-100 treatments, respectively, and by 27% and 54% in drought-stressed plants. Across all Cd treatments in both climates, drought stress cut transpiration by 47% ($p < 0.05$) on average.

Unlike all other parameters, the C_i/C_a of WW plants increased significantly by 15% and 26% in Cd-50 and Cd-100 treatments under CC conditions and by 20% in Cd-100 treatment under FC conditions. DS plants increased their C_i/C_a ratio by 25% and 82% in Cd-50 and Cd-100 treatments under CC conditions and by 16% and 24% under FC conditions, respectively (Fig. 3 C and 5A-D). C_i/C_a mainly did not differ between climates in the regular soil water regime. However, in the water stress regime, it was consistently higher under FC conditions in Cd-0 –Cd-50 treatment by 38%, on average. Drought stress significantly reduced C_i/C_a across all Cd treatments by 39% and 25%, on average, respectively, under CC and FC conditions. WUE of WW plants decreased by 23% in Cd-50 treatment under CC conditions and by 59% and 34% in Cd-100 treatment under CC and FC conditions, respectively. DS plants

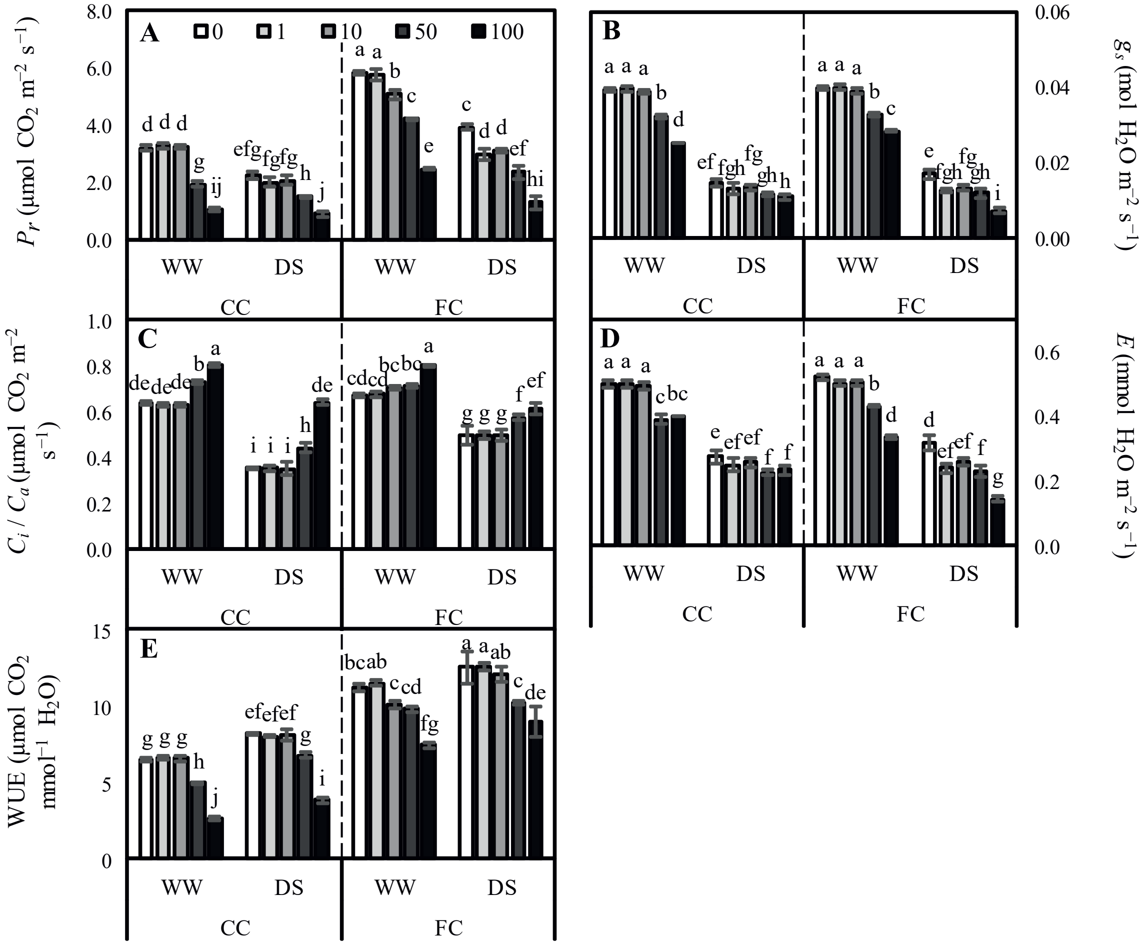

Fig. 3. Leaf gas exchange of rapeseed grown under different soil Cd concentrations (0, 1, 10, 50, and 100 mg kg^{-1}), climate conditions (CC: current climate, FC: future climate), and soil moisture levels (WW: well-watered, DS: drought-stressed). A: Photosynthetic rate (P_r); B: Stomatal conductance (g_s); C: The ratio of intercellular to ambient CO$_2$ concentration (C_i/C_a); D: Transpiration rate (E); E: Water use efficiency (WUE). Data are means ± SE (n = 9). Different letters over the bars indicate significant differences among treatments ($p < 0.05$).

decreased their WUE by 18% in Cd-50 treatment under both climates and 53% and 29% in Cd-100 treatment under CC and FC conditions, respectively (Figs. 3E and 5A-D). Both drought stress and FC conditions increased WUE, compared to regular water regime and CC conditions, especially in Cd-100 treatment.

Cd, soil moisture, and Cd × climate significantly affected all chlorophyll fluorescence (ChlF)-related parameters. Climate had a significant effect only for SFI$_{abs}$ and φPo, and the interactions of climate × soil moisture and all three factors significantly affected only φPo (Table S1). The detrimental effect of cadmium on the ChlF-related parameters describing the performance of photosynthetic apparatus, which are visualized on the radar plots as a percentage change from their respective controls (Cd-0 ones), was also most pronounced only in high Cd treatments under both climates and soil moisture levels (Figs. 4A-D and 5A-D). However, Cd less affected all ChlF-related parameters of both well-watered and drought-stressed rapeseed under FC than CC conditions. Meanwhile, when comparing DS plants to WW ones in both climates, high Cd treatments had less effect on all ChlF-related parameters under drought conditions.

To better systematize the response of growth, gas exchange, and ChlF-related parameters to Cd-induced stress, we created the clustered heatmaps for well-watered and drought-stressed rapeseed grown under CC and FC conditions (Fig. 5A-D). A dendrogram of Cd treatments highlighted the difference between these parameters under CC and FC conditions, especially in the regular water regime. In well-watered plants, under CC conditions, the treatments with lower Cd concentrations (Cd-1 and Cd-10) fell into one group with control plants (Cd-0), with Cd-0 and Cd-1 being more related to each other, treatments with high Cd concentrations (Cd-50 and Cd-100) formed another cluster (Fig. 5A). Meanwhile, under FC conditions, distinct groups were formed for Cd-0 and Cd-1 treatments and Cd-10 and Cd-50 treatments, leaving Cd-100 in a separate cluster (Fig. 5B). These differences between climates were determined by (1) less influenced growth, P_r, C_i/C_a, WUE, and ChlF-related parameters, especially PIabs, PItotal, and SFIabs, under FC conditions in Cd-50 treatment (Fig. 2 A, B, 3 A, C, E, and 4 A, B); (2) the contrasting response of several ChlF-related parameters, particularly PItotal, in Cd-10 treatment when, under CC and FC conditions, they were increased and decreased, respectively (Fig. 4 A, B); and (3) more decreased shoot DW, P_r, and WUE compared to their respective control under FC conditions in Cd-10 treatment (Fig. 2 A and 3 A, E). In drought-stressed plants, under CC conditions, separate clusters were formed for Cd-0 and Cd-10 treatments and Cd-1 and Cd-50 treatments because several ChlF-related parameters (i.e., PIabs, PItotal, and SFIabs) were more affected in Cd-1 than Cd-10 treatment (Fig. 4 C and 5 C). Meanwhile, under FC conditions, due to lower ChlF-related parameters, except for δRo and φRo, values in Cd-10 than in Cd-50 treatment compared to Cd-0, Cd-100 was more correlated with Cd-10 (Figs. 4D and 5D).

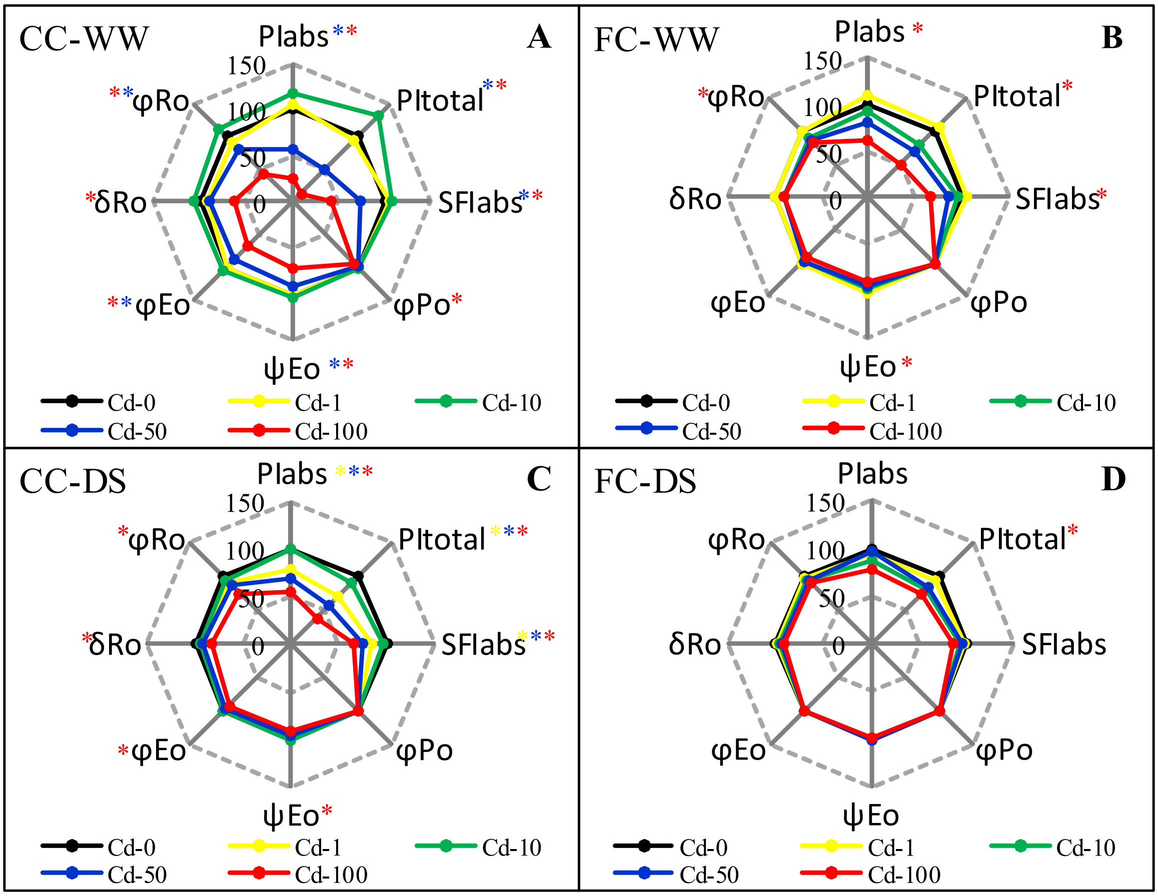

Fig. 4. JIP-test parameters (Performance indexes on an absorption basis: PIabs, PItotal, and SFIabs; Quantum yields and efficiencies for photochemistry: φPo, ψEo, φEo, δRo, and φRo) normalized on radar plots. A and B: Cd effect on well-watered (WW) rapeseed plants under current climate (CC) and future climate (FC) conditions (CC-WW and FC-WW, respectively); C and D: Cd effect on drought-stressed rapeseed plants under CC and FC conditions (CC-DS and FC-DS, respectively). Each curve represents the average of three measurements per treatment. Under all growing conditions, the status of Cd-stressed plants (Cd-1, Cd-10, Cd-50, and Cd-100) is shown relative to the status of Cd-untreated plants (Cd-0), expressed as 100% (*black line*). Asterisks, colored with the same color as the Cd treatment, mark significant differences from the respective controls (Cd-0 ones) (Fisher's LSD, $p < 0.05$).

3.4. Impact of climate and soil moisture conditions on macro and micronutrient concentrations in B. napus shoots and roots in response to Cd stress

High Cd soil concentrations of 50 and 100 mg kg^{-1} induced significant and prominent changes in the majority of macro and micronutrient concentrations in rapeseed shoots and roots (Figs. 6A-J, 7A-H, and 8A-D). Cd significantly affected all macro and micronutrient concentrations, except P, in shoots and roots (ANOVA, Table S2). The macro and micronutrient concentrations in rapeseed shoots and roots were less affected by climate and soil moisture conditions than Cd. Nevertheless, the interactions between these factors (Cd × climate, Cd × soil moisture, and climate × soil moisture) were mainly significant in micronutrient concentrations in shoots and roots. Meanwhile, the interaction of all three factors more affected macronutrient concentrations in shoots and roots (Table S2).

The most noticeable changes in macronutrient concentrations in shoots occurred in K, Mg, and S concentrations, which increased significantly under CC conditions at both soil moisture levels in Cd-50 and Cd-100 treatments. Under FC conditions, K concentration increased at both soil moisture levels but only in the Cd-100 treatment. Mg and S concentrations increased significantly in the Cd-100 treatment in well-watered conditions and the Cd-50 and Cd-100 treatments in the water stress regime. Ca concentration changed significantly only under CC conditions when increased significantly in WW plants under both high Cd treatments, while P concentration did not change remarkably under any conditions (Figs. 6A-E and 8A-D).

The most notable changes in macronutrient concentrations in roots occurred in WW plants under CC conditions, where all of them increased significantly in high Cd treatments, except P in Cd-50. Under FC conditions, P concentration in WW plants decreased in both high Cd treatments, while Ca, Mg, and S concentrations increased only in the Cd-100 treatment (Figs. 6F-J and 8A-D). DS plants under CC conditions showed higher Mg concentration in both high Cd treatments, while Ca and S concentrations significantly increased only in the Cd-100 treatment, and P concentration in Cd-100 decreased. Meanwhile, DS plants under FC conditions had higher P and Mg concentrations in the Cd-50 treatment, higher S concentration in Cd-100, and higher K concentration in both high Cd treatments.

Differentially from other micronutrients, Cu concentration in shoots significantly decreased in Cd-50 and Cd-100 treatments in WW plants and Cd-100 treatment in DS plants under CC conditions. It also was lower under FC conditions in Cd-100 treatment at both soil moisture levels. Meanwhile, all other micronutrient concentrations in shoots increased in high Cd treatments (Figs. 7A-D and 8A-D). Under CC conditions, Fe and Zn concentrations increased significantly in both high Cd treatments at both soil moisture levels, while Mn concentration increased in the Cd-50 treatment. Under FC conditions, WW plants had higher Fe, Mn, and Zn concentrations in the Cd-100 treatment, whereas DS plants showed higher Fe and Mn concentrations in the Cd-50 treatment and Zn in the Cd-100 treatment.

Under CC conditions, all micronutrient concentrations increased

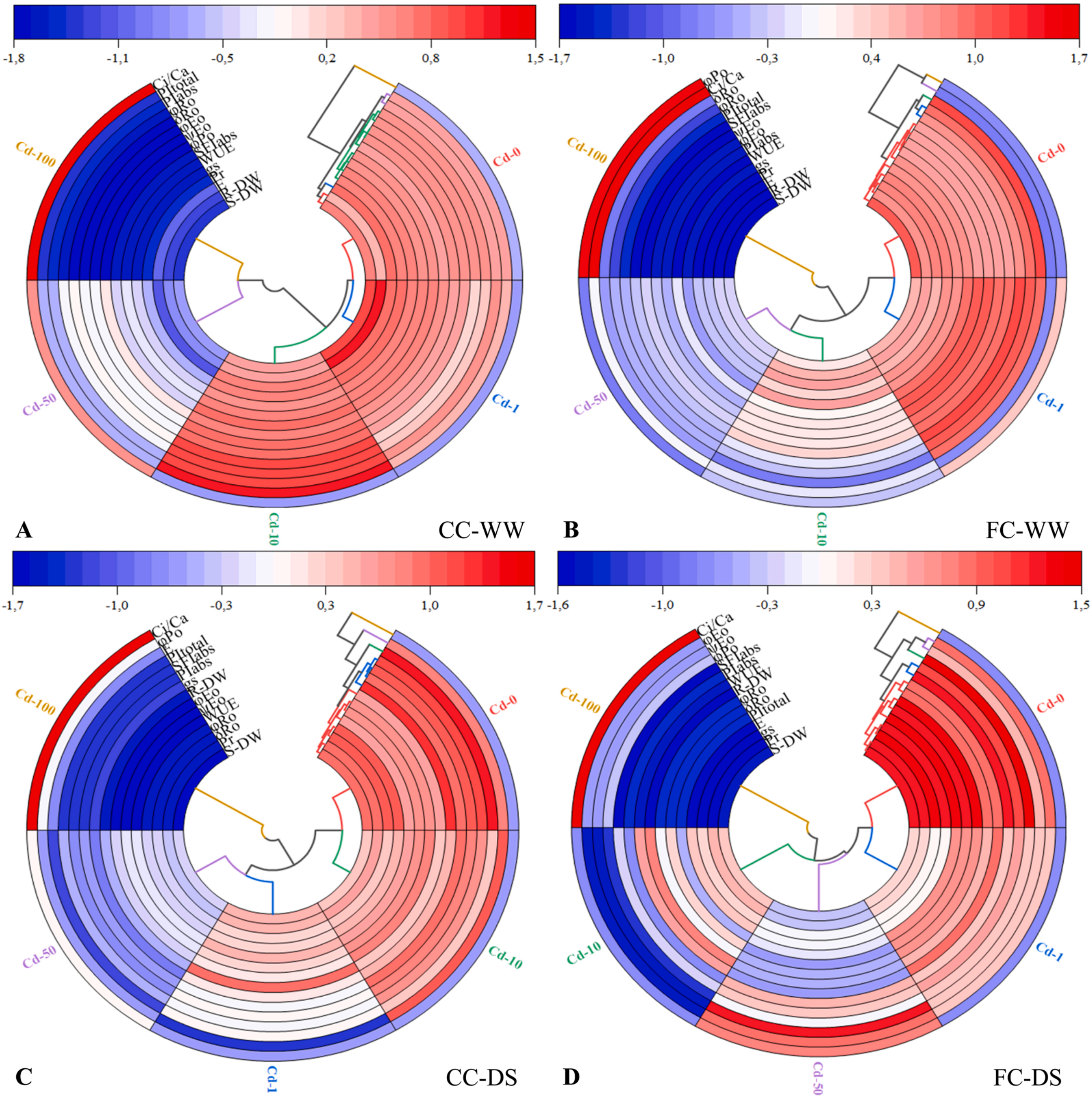

Fig. 5. Polar heatmap with dendrogram of growth, gas exchange, and ChlF-related parameters of rapeseed grown under different soil Cd concentrations (0, 1, 10, 50, and 100 mg kg^{-1}, designated as Cd-0, Cd-1, Cd-10, Cd-50, and Cd-100) in well-watered (WW) conditions under the current climate (CC) and future climate (FC) (A and B, respectively) and drought-stressed (DS) conditions under CC and FC (C and D, respectively).

significantly in the roots of the well-watered plants in high Cd treatments. In drought-stressed plants grown under CC conditions, Zn concentration increased in both high Cd treatments, while Fe, Mn, and Cu concentrations increased only in Cd-50. Under FC conditions, however, none of the micronutrient concentrations significantly differed in the Cd-100 treatment versus Cd-0, while only Fe concentration was reduced in the Cd-50 treatment. Meanwhile, in DS plants, Mn and Cu concentrations in the Cd-50 treatment increased significantly, Fe concentration in the Cd-100 treatment decreased, and Zn concentration decreased in both high Cd treatments (Figs. 7E-H and 8A-D).

Hierarchical clustering analysis for macro and micronutrient concentrations in rapeseed shoots and roots also showed more difference in well-watered than drought-stressed plants (Fig. 8A-D). In well-watered plants, separate clusters formed for Cd-0 –Cd-10 treatments, with Cd-1 and Cd-10 being more related to each other, and another for Cd-50 and Cd-100 treatments under CC conditions (Fig. 8A). Meanwhile, under FC conditions, Cd-50 treatment formed a group with Cd-0 –Cd-10 treatments, leaving Cd-100 in a single cluster (Fig. 8B), as the significant macro and micronutrient concentration impairments in shoots and roots mainly were manifested only in Cd-100 treatment (Figs. 6F-J and 7E-H). In drought-stressed plants, under both CC and FC conditions, Cd-0 –Cd-10 treatments formed one group, and Cd-50 and Cd-100 treatments another (Fig. 8C, D). The only difference between climates occurred in the Cd-0 –Cd-10 cluster when, under CC conditions, Cd-0 and Cd-1

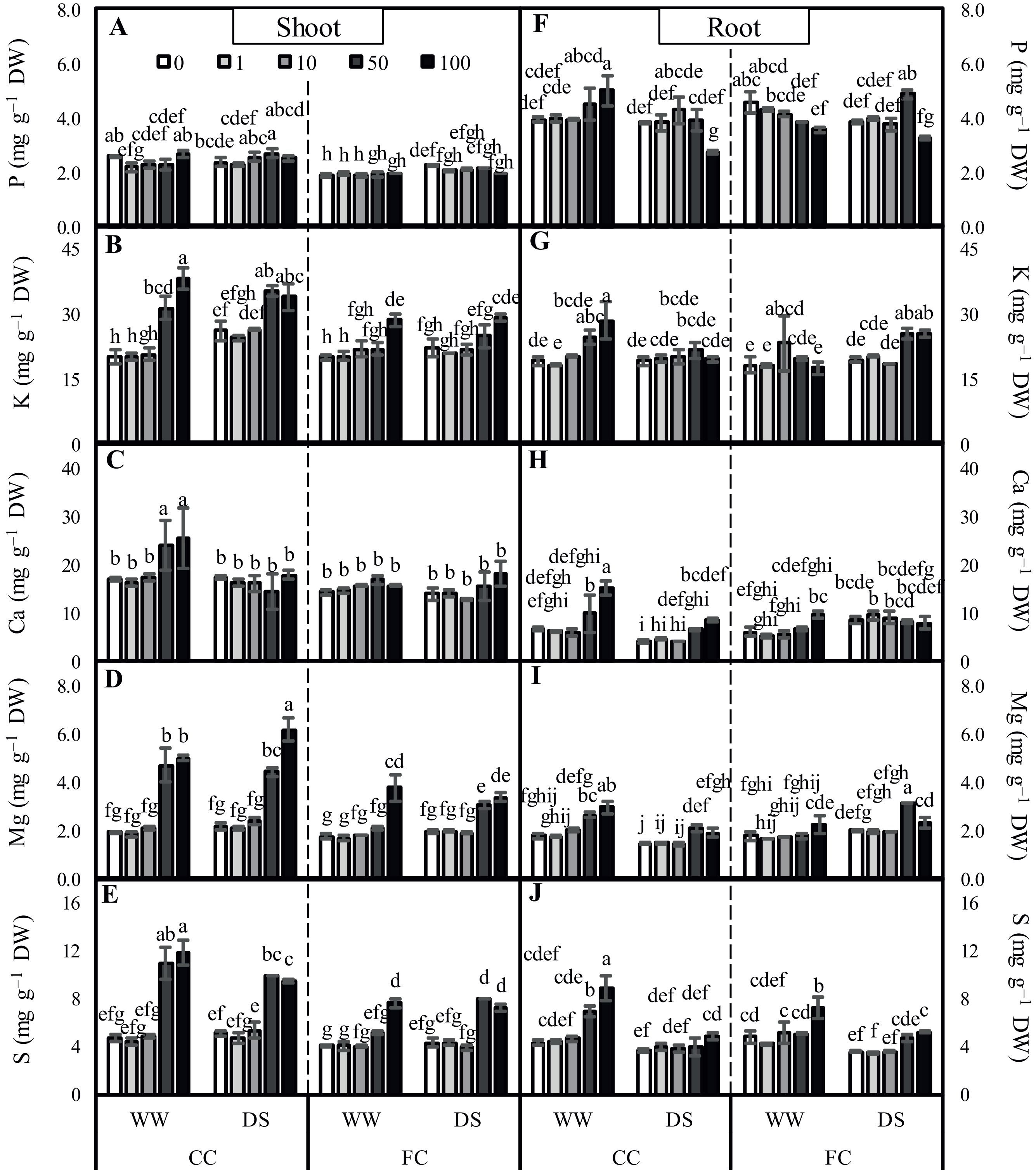

Fig. 6. Macronutrient concentrations in rapeseed shoots (left panels) and roots (right panels) grown under different soil Cd concentrations (0, 1, 10, 50, and 100 mg kg^{-1}), climate conditions (CC: current climate, FC: future climate), and soil moisture levels (WW: well-watered, DS: drought-stressed). A and F: Phosphorus (P); B and G: Potassium (K); C and H: Calcium (Ca); D and I: Magnesium (Mg); E and J: Sulphur (S). Data are means ± SE (n = 9). Different letters over the bars indicate significant differences among treatments ($p < 0.05$).

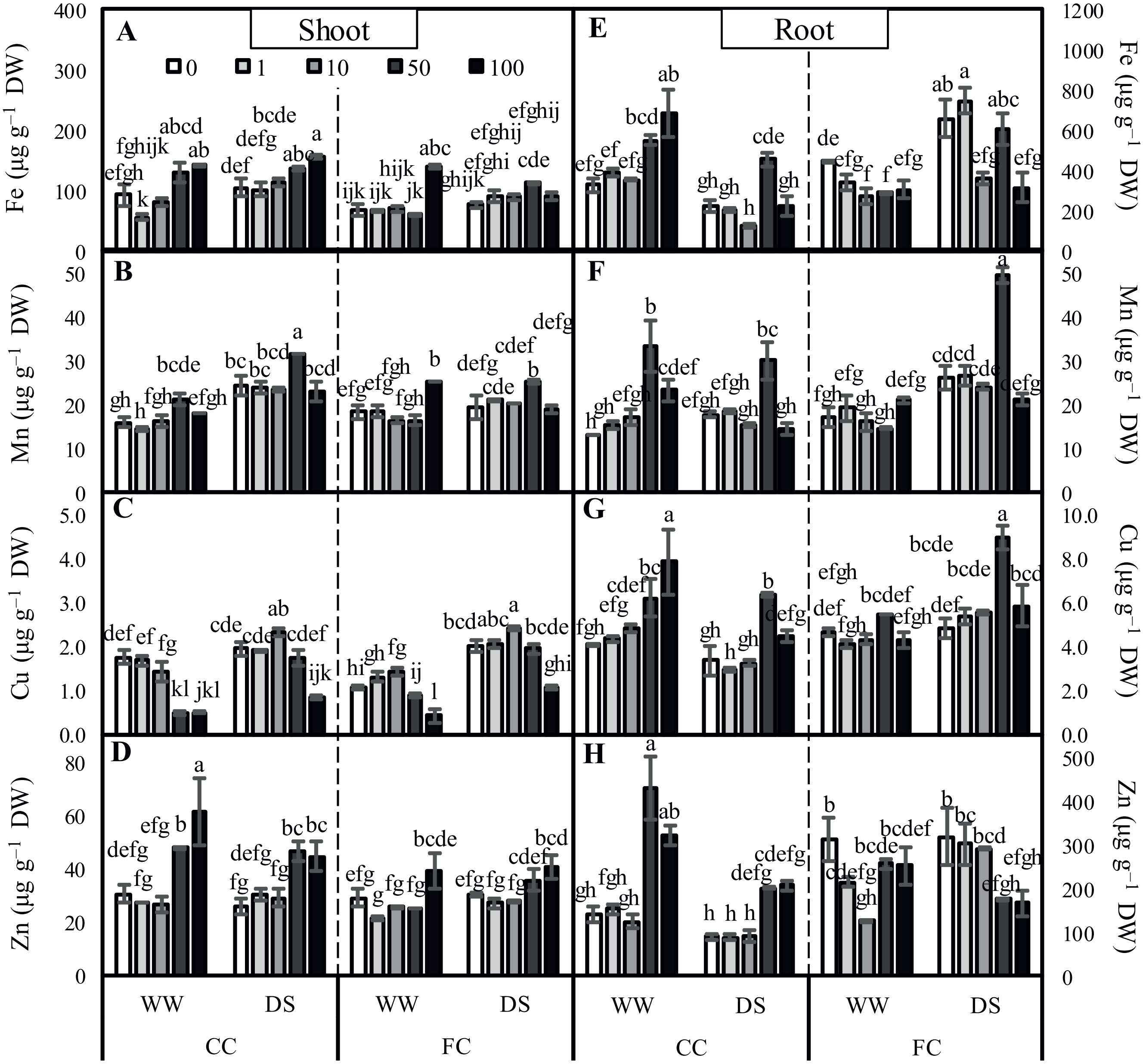

Fig. 7. Micronutrient concentrations in rapeseed shoots (left panels) and roots (right panels) grown under different soil Cd concentrations (0, 1, 10, 50, and 100 mg kg^{-1}), climate conditions (CC: current climate, FC: future climate), and soil moisture levels (WW: well-watered, DS: drought-stressed). A and E: Iron (Fe); B and F: Manganese (Mn); C and G: Cuprum (Cu); D and H: Zinc (Zn). Data are means ± SE (n = 9). Different letters over the bars indicate significant differences among treatments ($p < 0.05$).

treatments were more closely related, while, under FC conditions, more correlated were Cd-1 and Cd-10 treatments.

4. Discussion

4.1. Impact of climate and soil moisture conditions on Cd-phytoextraction efficiency by B. napus

Most plants exhibit visible Cd toxicity symptoms when Cd concentration in plant tissue reaches 3–30 mg kg^{-1} [18]. Both well-watered (WW) and drought-stressed (DS) rapeseed plants exceeded this level in high Cd treatments of 50 and 100 mg kg^{-1} (Fig. 2 C, D) exhibiting the visible toxicity symptoms as well. As future climate conditions (FC) resulted in lower aboveground tissue Cd concentration than under current climate (CC) conditions (Fig. 2 C), fewer visible Cd toxicity symptoms on the leaves were manifested as well (Fig. 1A-D). Therefore, the present study's findings indicate that *B. napus* tolerance to high Cd concentrations improved under FC conditions with elevated temperature and CO_2 concentration regardless of soil moisture levels, mainly owing to lower Cd shoot concentration (Fig. 2 C). This concentration dilution effect caused by faster plant growth and higher biomass production could also be seen comparing WW and DS plants (Fig. 2 A, C) and was confirmed by a strong negative correlation between shoot dry weight (DW) and shoot Cd concentration (Fig. 9A-D). The dilution phenomenon is frequently observed under elevated CO_2 conditions [41, 55], but it can also be seen under elevated temperature conditions when the growth of different plant parts exceeds their rate of metal uptake [54].

Slightly higher bioconcentration factor values in drought-stressed plants compared to well-watered plants and overall lower BCF values

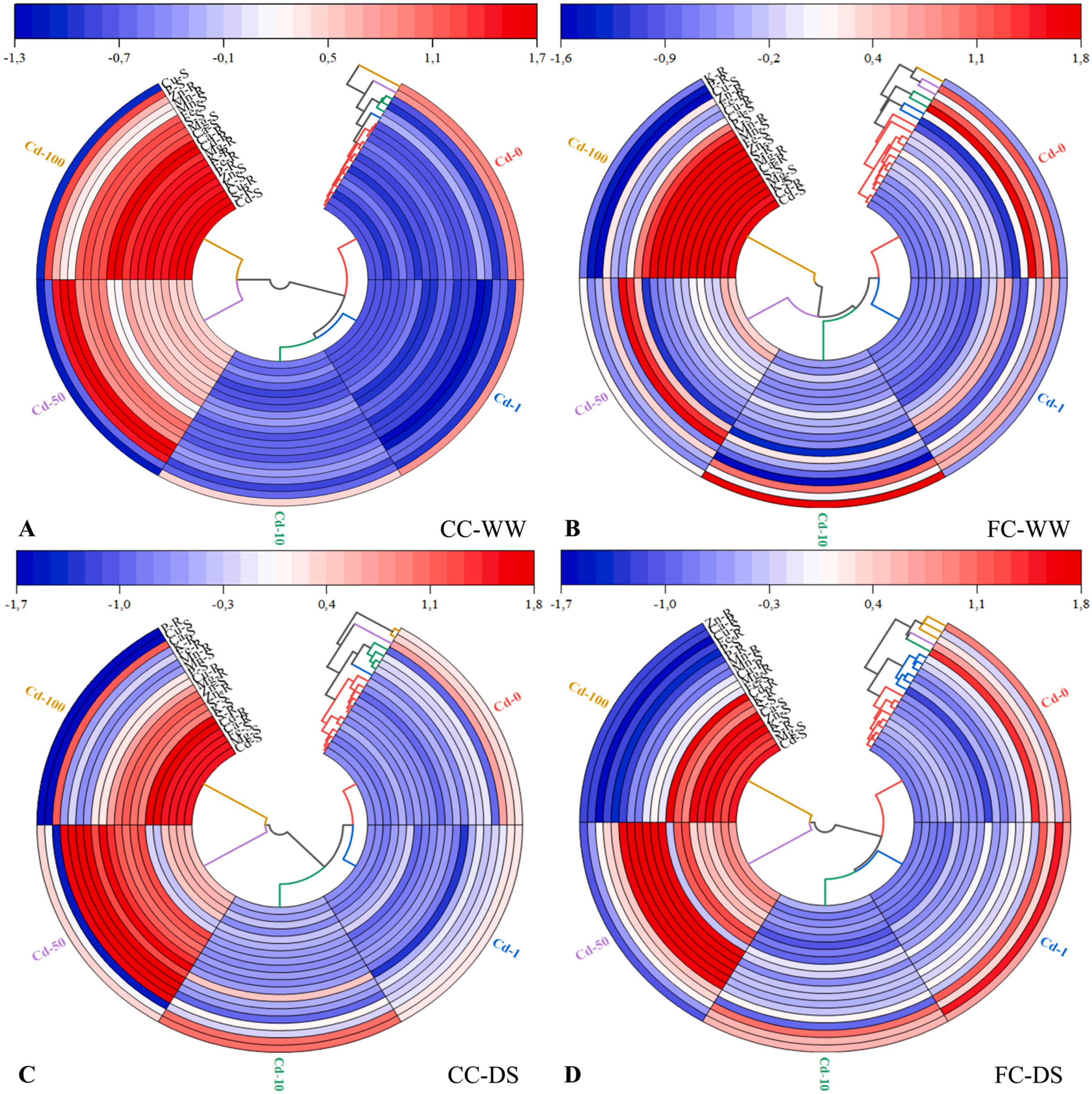

Fig. 8. Polar heatmap with dendrogram of Cd and macro and micronutrient concentrations in shoots and roots of rapeseed grown under different soil Cd concentrations (0, 1, 10, 50, and 100 mg kg^{-1}, designated as Cd-0, Cd-1, Cd-10, Cd-50, and Cd-100) in well-watered (WW) conditions under the current climate (CC) and future climate (FC) (A and B, respectively) and drought-stressed (DS) conditions under CC and FC (C and D, respectively). The abbreviations 'S' and 'R' stand for shoot and root, respectively.

under FC versus CC conditions (Table 2) were also related to concentration and dilution phenomena, respectively, with significant negative correlation between shoot DW and BCF ($r = -0.63$, $p < 0.001$). On the other hand, Cd accumulation in shoots positively correlated with shoot DW from high Cd treatments ($r = 0.71$, $p = 0.002$). Even though BCF is regarded as the key indicator for assessing plants' ability to extract heavy metals [36], it does not permit the assessment of overall phytoextraction potential. Therefore, aboveground biomass production was the primary factor causing significantly higher shoot Cd accumulation and removal afterward (Table 2, Fig. 9A-D). In addition, the soil Cd removal rate (%) showed the opposite trends than BCF did (Table 2), exhibiting a strong positive relationship with shoot DW ($r = 0.83$, $p < 0.001$). As a result, because metal removal efficiency is determined by the amount of metal extracted in the aboveground biomass [95], the overall HM accumulation in non-hyperaccumulator plants, as *B. napus*, with high aboveground biomass production can be comparable to hyperaccumulators, despite their lower metal-accumulating capacities [4,101]. This finding further supports the concentrations and dilution phenomena observed under drought and FC conditions, respectively, and indicates the higher rapeseed potential for Cd phytoextraction under FC than in CC conditions at both soil moisture levels. Only Cd-50 treatment in the regular water regime, on the other hand, resulted in a

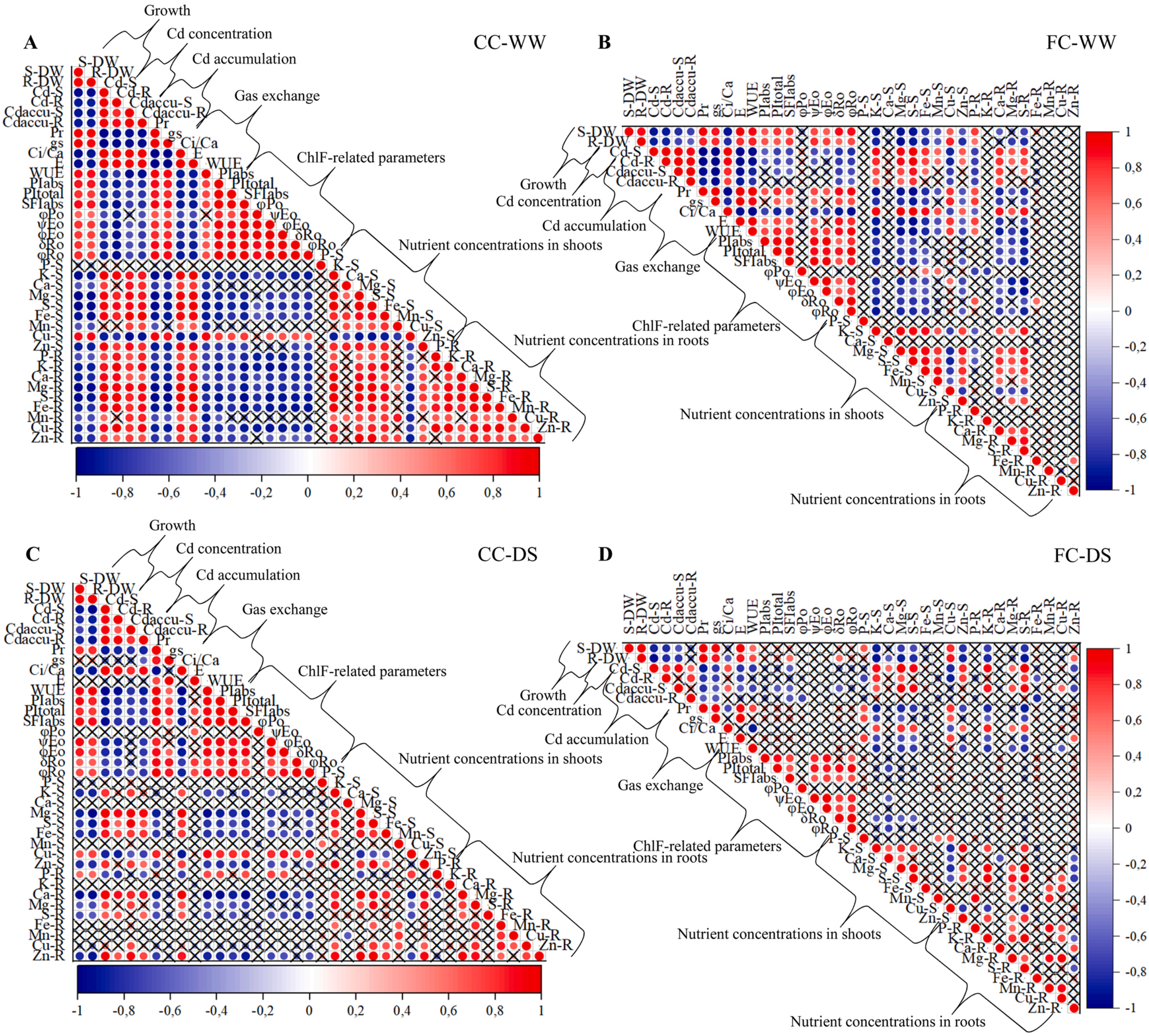

Fig. 9. Correlation matrixes among the measured rapeseed growth and physiological traits, Cd concentration and accumulation in shoots and roots, and nutrient concentrations in shoots and roots in well-watered (WW) conditions under the current climate (CC) and future climate (FC) (A and B, respectively) and drought-stressed (DS) conditions under CC and FC (C and D, respectively). The size and intensity of red (positive) and blue (negative) circles are mapped with Pearson's correlation coefficient values ($p < 0.05$) with stronger correlations being larger and darker than weaker ones. The correlations that are not significantly related across are marked on the symbol 'x'. The abbreviations '-S' and '-R' stand for shoot and root, respectively.

significantly higher Cd removal rate under FC conditions of up to 65% (Table 2). This is consistent with the clustering analysis, which showed that the physiological status of well-watered plants improved under FC conditions in Cd-50 treatment, as the clustering of Cd-50 with Cd-100 treatment under CC conditions was switched to clustering with Cd-0 –Cd-10 treatments under FC conditions in the polar heatmaps with dendrogram of growth, gas exchange and ChlF-related parameters and macro and micronutrient concentrations in rapeseed shoots and roots (Figs. 5A, B and 8A, B).

4.2. *Impact of climate and soil moisture conditions on photosynthetic performance and nutritional status of B. napus in response to Cd stress*

The accumulation of Cd in plants is well known to disrupt the uptake of important nutrients such as calcium, magnesium, potassium, and others, as well as water uptake [32,34,62,79], which was also a case in this study (Figs. 6A-J, 7A-H, and 8A-D). These impairments hands down the onset of visible Cd phytotoxicity symptoms, the most notable of which is leaf chlorosis, resulting from the destruction of the chloroplast ultrastructure and the impairment of chlorophylls production, which in turn cause the reduction in photosynthetic rate [32,79]. Matching the chlorosis symptoms (Fig. 1A-D), the photosynthetic rate (P_r), which followed the trend of shoot DW production (Fig. 2 A, 3 A, and 5A-D) with a very strong positive relationship between them (Fig. 10A-D), was more impaired by Cd under current than future climate conditions. However, the reduction of P_r was more noticeable in the water stress regime under both CC and FC conditions, unlike the symptoms of chlorosis (Figs. 1A-D and 3 A), implying additional restrictions to photosynthesis under drought conditions to those of Cd-induced disturbance in mineral nutrient balance. This discrepancy could be explained by the fact that stomatal conductance (g_s), the intercellular to ambient CO_2 concentration (C_i/C_a), and transpiration (E) were also

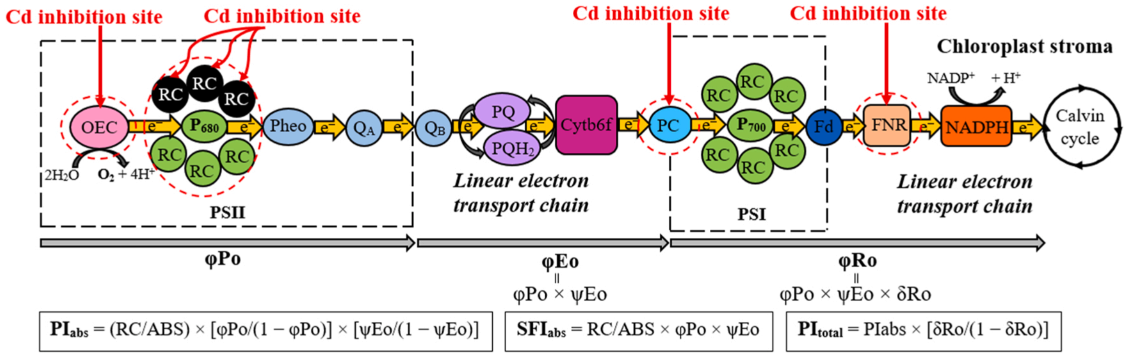

Fig. 10. A simplified schematic representation of the possible sites of Cd inhibition in the photosynthetic linear electron (e^-) transport chain in *B. napus* plants. The main inhibition sites are the Mn_4Ca cluster of the oxygen-evolving complex (OEC), the deactivation of some fraction of PSII RCs, the stretch between Cytb6f and PSI due to a lack of PC caused by Cd-induced Cu deficiency, and the acceptor side of PSI due to the inactivation of FNR. Electron transport chain components: OEC, oxygen evolving complex, PSII and PSI, photosystem II and photosystem I; RC, reaction center; P_{682}, exited state of PSII RC, which is the primary electron donor of PSII; Pheo, pheophytin; Q_A, a primary quinone electron acceptor of PSII; Q_B, a secondary quinone electron acceptor of PSII; PQ, plastoquinone; PQH_2, a reduced form of Q_B that leaves PSII, Cytb6f, cytochrome b6f complex; PC, plastocyanin; Fd, ferredoxin; FNR, ferredoxin-NADP$^+$-reductase; NADPH, reduced nicotinamide adenine dinucleotide phosphate; P_{700}, exited state of PSI RC, which is the primary electron donor of photosystem I.

decreased in the water stress regime, compared to the regular soil moisture (Fig. 3A-D), suggesting a direct drought stress-induced stomatal limitation to photosynthesis. Moreover, g_s, C_i/C_a, and E all possessed a very close positive relationship with P_r ($r = 0.826 - 0.996$, $p < 0.05$) across all Cd treatments, except in Cd-100 under CC conditions. It is well recognized that almost all plants' primary and paramount response to the lack of soil moisture is rapid stomatal closure to prevent further water loss through transpiration. This physiological adaptation allows plants to maintain hydraulic function but limits CO_2 entry into the leaves, resulting in reduced CO_2 assimilation [104,12,13,22]. In addition, the decrease in photosynthetic rate under drought conditions could be directly linked to increased water use efficiency (Fig. 3E), which is also a common plant response to drought stress caused by stomatal reduction [12,13,17,20] as a result of osmotic imbalance [51]. Meanwhile, despite a significant decrease in g_s, C_i/C_a increased in high Cd treatments under both climates and soil moisture levels (Fig. 4B, C), displaying a strong negative correlation with P_r (Fig. 9A-D). These results indicate that, unlike drought, the adverse effect of cadmium on rapeseed photosynthetic performance was attributed to non-stomatal restriction rather than stomatal limitation, which is in agreement with the findings of other studies [5,82,83].

The primary site of Cd action through non-stomatal limitations is the photosynthetic apparatus, especially the light-harvesting complex II and both photosystems (PSI and PSII) [32,34]. It has been shown that Cd interrupts the photosynthetic electron transfer (ET) and lowers the efficiency of energy conversion in photosystem II [66], which is in line with our findings (Fig. 4A-D). Our results showed that at both soil moisture levels under CC conditions high Cd concentrations, especially Cd-100 treatment, disrupted the entire electron transport chain, decreasing all the electron transport-related quantum yields as well as intermediate energy transduction efficiencies with the effect being larger in the sequence $\varphi Ro > \delta Ro > \varphi Eo > \psi Eo > \varphi Po$ (Fig. 4 A, C). Moreover, all these quantum yields and efficiencies, except φPo in the water stress regime, had a moderate to strong positive relationship with P_r (Fig. 9 A, C). Similar results were found in the study of Yusuf et al. [103] with wild-type *B. juncea* plants. Furthermore, the structure-function index (SFI_{abs}), which is the product of terms of three independent parameters (RC/ABS, the density of active PSII reaction centers on Chl *a* basis, φPo, and ψEo), and the performance indexes on an absorption basis (PI_{abs} and PI_{total}) were all diminished in high Cd treatments, particularly Cd-100. Their reduction showed a very strong positive correlation with P_r, except in the water stress regime under FC conditions (Fig. 9A-D) and was much more pronounced under CC conditions (Fig. 4A-D). SFI_{abs} provides structural and functional information about the strength of the influence of internal factors promoting the reactions in PSII that "favor" photosynthesis [30,60,87]. Meanwhile, PI_{abs} and PI_{total} are the products of terms expressing partial potentials for energy conservation at the sequential energy bifurcations from exciton to the reduction of intersystem electron acceptors and to the reduction of the end acceptors of photosystem I, respectively [89,103]. Therefore, the significantly lower values of SFI_{abs} and PI_{abs} reflect inefficient use of absorbed light energy due to the increased density of inactive PSII reaction centers, which resulted in less excitation energy being transformed into chemical energy that is further directed to biochemical processes of photosynthesis, as in some part was previously suggested by Franić et al. [25]. Meanwhile, an even higher reduction in PI_{total} reflects Cd-induced damage to both PSII and PSI, with the latter resulting from the decrease in δRo, which, according to Schansker et al. [78], indicates a decrease in electron flow at the acceptor side of PSI caused by ferredoxin-NADP$^+$-reductase (FNR) inactivation. The lower degree of reduction in SFIabs, PIabs, and PItotal in drought-stressed plants compared to well-watered plants (Fig. 4A-D) could be attributed to the darker green color of DS plants and fewer chlorosis symptoms, particularly under FC conditions (Fig. 1A-D). However, due to both stomatal and non-stomatal constraints of photosynthesis under the simultaneous presence of Cd and drought, P_r, shoot DW, and shoot Cd accumulation of drought-stressed plants under FC conditions were all significantly lower, compared to well-watered plants (Fig. 2 A, E and 3 A).

WUE is defined as the ratio of water used by the plant for metabolism to water lost through transpiration [74]. Therefore, a decrease in WUE in response to high Cd treatments (Fig. 3E) implies that, unlike drought stress, Cd had a greater influence on rapeseed photosynthesis than water balance. Along with the found moderate to strong positive correlation between WUE and P_r under both climate and soil moisture conditions (Fig. 9A-D), these findings further support the presumption of non-stomatal constraints rather than stomatal limitations to photosynthesis under Cd stress. However, decreased transpiration rate at high Cd soil concentrations may have further exacerbated the growth inhibition, as it could reduce mineral nutrients translocation into aboveground parts [34]. Regarding the mineral nutrients, their concentrations in shoots and roots also mainly reflected the concentration and dilution phenomena. The increases in the majority of analyzed macro and micronutrients in the shoots and roots in Cd-50 and Cd-100 treatments point out the concentration effect when the shoot and root DW were highly decreased under both climates and soil moisture levels. Meanwhile, at both soil moisture levels, less elevated macro and micronutrient concentrations under FC compared to CC conditions in high Cd soil concentrations make a note of the dilution effect due to less decreased shoot and root biomasses (Figs. 6A-J, 7A-H, and 2 A, B). Moreover, unlike shoot and root DW, Cd concentration and accumulation in shoots and roots showed a significant positive correlation with the majority of macro and micronutrient concentrations in shoots and roots, particularly under CC conditions in the regular water regime. Only Cu concentration in shoots had a negative relationship with Cd concentration in shoots and roots under CC and FC conditions at both soil moisture levels (Fig. 9A-D).

The deficiency in mineral nutrients in distinct plant organs is frequently observed alongside Cd uptake [35,59,62], as Cd enters plant cells primarily through cation channels of Ca, Zn, Fe, Mn, K, or transporters of other divalent cations [52,62,9]. For example, leaf chlorosis was observed in *Arabidopsis thaliana* after Cd exposure, primarily due to Cd-induced iron (Fe) deficiency in the shoots [99], which could be linked to reduced chlorophyll synthesis [48]. A lack of zinc (Zn) also causes chlorotic areas on the leaves, necrosis, and mid-leaf collapse, which could affect physiological and genetic parameters such as growth, enzyme activity, protein production, and defense mechanisms, resulting in cellular and physical damage [75]. In addition, Fe deficiency affects photosynthetic electron transport, which has a very high demand for Fe cofactors, whit the highest demand for iron–sulfur (Fe–S) clusters [47]. Photosystem I subunits require three 4Fe-4S clusters, each Rieske subunit of the cytochrome b6f (Cytb6f) complex requires two 2Fe-2S clusters, and ferredoxins (Fds) requires two 2Fe-2S clusters [26,37,7]. The Cytb6f complex contains multiple heme cofactors for electron transport and exists as a dimer, spanning the subunits with a total of 12 Fe atoms [61]. Photosystem II also contains a cytochrome heme cofactor with photoprotective properties [61]. However, PSI is more affected by Fe deficiency than PSII [47]. Sulfur (S) is also an important structural component of many co-enzymes and prosthetic groups, including ferredoxins, which are required for N assimilation [77]. Potassium (K) is involved in many physiological processes, including photosynthesis and regulation of opening and closing of the stomata [72]. K has been shown to play a significant role in the maintenance of chlorophyll fluorescence in plants treated with Cd, by retaining a portion of active RCs and ensuring a complete reduction of the plastoquinone pool [63].

A higher level of cellular Cd either interferes with Mg^{2+} insertion into protoporphyrinogen or may cause chlorophylls destruction due to Mg^{2+} substitution in both chlorophyll *a* and chlorophyll *b* [28]. These could have a significant impact on photosynthesis because such chlorophylls may have far lower fluorescence quantum yields than Mg-chlorophylls [48]. Cd can also bind competitively to the Ca-binding sites in the catalytic center in photosystem II, inhibiting photoactivation of the water-splitting complex [23] with the possible direct suppression of oxygen evolution [64]. It has been shown that Cd induces changes in the Mn_4Ca cluster of the oxygen-evolving complex (OEC) [14,102]. Since the OEC is located on the PSII donor side [31], it means that Cd-induced changes in the Mn_4Ca cluster inhibit efficient electron donation from the PSII donor side to oxidized PSII RCs at the PSII acceptor side [85], as the electron flow to the acceptor side exceeds the electron flow from the donor side [31]. A downfall in the electron donation from OEC to the oxidized PSII RCs under Cd exposure was recently shown with maize plants in the study of Janeeshma et al. [40]. However, Cd can also decrease the electron transfer rate from Q_A to Q_B (i.e. from primary to secondary quinone electron acceptor of PSII) due to interaction with non-heme Fe and conformational modification of Q_B pocket [65]. Therefore, both the donor side (Mn4Ca cluster) and the acceptor side (Q_A and Q_B) of PSII are considered to be Cd-sensitive sites [91]. In addition, stomatal closure caused by Cd entry into guard cells in competition with Ca^{2+} [67] and a decrease in stomata number per unit area can occur in response to Cd stress, resulting in lower conductance to CO_2 [68].

Considering the concentration effect, our findings revealed that, among all the macro and micronutrients, the most affected by Cd was Cu accumulation in shoots. Cu is an important constituent of plastocyanin (PC) [80], which is involved in electron transport between the cytochrome b6f complex and photosystem I [15]. The Cytb6f complex is a central component of photosynthetic electron transport chain, which couples electron transfer between PSII and PSI by oxidizing a reduced form of secondary plastoquinone electron acceptor, Q_B, that leaves PSII (PQH_2) and reducing PC (Malone et al., 2021; [93]). Severe Cu deficiency may result in a defect in photosynthetic electron transport due to a lack of plastocyanin [16,80]. Therefore, dramatically decreased Cu concentration in shoots, particularly under CC conditions, might have been the result of Cd-induced disruption in photosynthetic electron transfer between Cytb6f complex and PSI. These results explain the higher reduction in φRo and δRo (quantum yield and efficiency of ET from PSII to PSI, respectively), which is dependent on electrons transferred from PQH_2 to PSI [60], compared to φEo, ψEo, and φPo (Fig. 4A-D). Moreover, at both soil moisture levels under CC conditions, a significant strong positive relationship was found between Cu concentration in shoots and all the photosynthetic transport and photosynthetic apparatus performance describing parameters, except for φPo (Fig. 9 A, C). A significant but negative strong relationship was also found between the majority of ChlF-related parameters and K, Mg, S, Fe, and Zn concentrations in shoots, especially under CC conditions in regular soil moisture (Fig. 9A-D).

The aforementioned possible alterations in the structure and function of the photosynthetic apparatus of plants under Cd stress, related to macro and micronutrient deficiency, may have occurred and influenced the overall *B. napus* photosynthetic performance in this study. The findings of this study imply that the significant PI_{total} reduction in response to high Cd soil concentrations under both climate and soil conditions may reflect the reduction in photosynthetic electron transport due to the closure of PSII reaction centers, functional impairment in the activity of OEC, the inactivation of FNR, and a lack of PC (Fig. 10). Therefore, the present study findings add to our understanding of Cd inhibition sites in the photosynthetic linear electron (e^-) transport chain, which was previously demonstrated by Parmar et al. [65] in an overview of the effects of Cd exposure to plants at various levels in photosynthetic machinery.

5. Conclusions

B. napus was found to be relatively resistant to Cd soil contamination up to 50 mg kg^{-1} when a significant reduction in their performance was recorded. A significant positive correlation between Cd plant accumulation and the majority of macro and micronutrient concentrations in shoots and roots highlighted the concentration phenomenon for mineral nutrients, which was more pronounced under CC conditions at both soil moisture levels. Among the nutrients, Cu was the most affected by Cd. Cu concentration in shoots decreased with Cd plant concentration under both climate and soil conditions and increased with most of photosynthetic transport and performance-describing parameters under CC conditions at both soil moisture levels. Growth retardation in Cd-50 and Cd-100 treatments was closely related to the decrease in photosynthetic rate (P_r), which was primarily due to the repression of electron transport and was much more pronounced under CC conditions at both soil moisture levels. The simultaneous presence of Cd and drought in the growth media caused both stomatal and non-stomatal constraints, significantly lowering P_r, shoot dry weight (DW), and shoot Cd accumulation of drought-stressed plants under FC conditions compared to well-watered plants. Therefore, the physiological status of only well-watered Cd-affected plants was significantly improved under FC conditions regarding increased photosynthetic performance, which was related to better mineral nutrient balance, resulting in higher Cd extraction efficiency in the Cd-50 and Cd-100 treatments. The soil Cd removal rate, which had a strong positive relationship with shoot DW and trended in the opposite direction as the bioconcentration factor, was also up to 65% ($p < 0.05$) higher in well-watered plants under FC conditions in Cd-50 treatment. Thus, this study clarified how the combined impact of the two most important climate change-related variables (elevated CO_2 and temperature) may affect the Cd extraction efficiency of *B. napus* grown at different soil moisture levels. Future research on gene expression in the promotion of Cd phytoremediation by regulating climate variables and soil conditions, alongside the relevant physiological and biochemical parameters, is required to fill the gaps in knowledge of Cd uptake mechanisms in *B. napus* at the molecular level.

Statement of “Environmental implication

Climate conditions, such as elevated CO_2, warming, and drought, may have a significant impact on plants growing in heavy metal polluted soil. Good adaptation to the prevailing environment may become the key plant feature, determining its phytoextraction potential. Cd is one of the most hazardous materials; however, the mechanisms involved in Cd accumulation under changing climate conditions have received little attention. Since the presence of Cd in growth media at the same time combined with all these climate change-related variables has not yet been investigated, we believe that this manuscript is appropriate for publication in the *Journal of Hazardous Materials*.

CRediT authorship contribution statement

Austra Dikšaitytė: Conceptualization, Funding acquisition, Data curation, Formal analysis, Investigation, Methodology, Visualization, Writing — original draft, Writing – review & editing. **Inesa Kniuipytė:** Data curation, Investigation.**Jūratė Žaltauskaitė:** Conceptualization, Investigation, Writing – review & editing.

Declaration of Competing Interest

The authors declare that they have no known competing financial interests or personal relationships that could have appeared to influence the work reported in this paper.

Data availability

No data was used for the research described in the article.

Acknowledgements

This research was funded by the European Social Fund under the No 09.3.3-LMT-K-712 “Development of Competences of Scientists, other Researchers and Students through Practical Research Activities” measure.

Appendix A. Supporting information

Supplementary data associated with this article can be found in the online version at doi:10.1016/j.jhazmat.2023.131181.

References

[1] Abbas, T., Rizwan, M., Ali, S., Adrees, M., Mahmood, A., Zia-Ur-Rehman, M., Ibrahim, M., Arshad, M., Qayyum, M.F., 2018. Biochar application increased the growth and yield and reduced cadmium in drought stressed wheat grown in an aged contaminated soil. Ecotoxicol Environ Saf 148, 825–833. https://doi.org/10.1016/j.ecoenv.2017.11.063.

[2] Al-Hamzawi, A.A., Al-Gharabi, M.G., 2019. Heavy metals concentrations in selected soil samples of Al-Diwaniyah governorate, Southern Iraq. SN Appl Sci. https://doi.org/10.1007/s42452-019-0892-7.

[3] Ali, E., Hussain, A., Ullah, I., Khan, F.S., Kausar, S., Rashid, S.A., Rabbani, I., Imran, M., Kakar, K.U., Shah, J.M., Cai, M., Jiang, L., Hussain, N., Sun, P., 2020. Cadmium phytotoxicity: issues, progress, environmental concerns and future perspectives. Rev la Fac Cienc Agrar 52 (1), 391–405.

[4] Ali, H., Khan, E., Sajad, M.A., 2013. Phytoremediation of heavy metals—Concepts and applications. Chemosphere 91, 869–881. https://doi.org/10.1016/j.chemosphere.2013.01.075.

[5] Andrade, W.V., de Oliveira Neto, C.F., dos Santos Filho, B.G., do Amarante, C.B., Cruz, E.D., Okumura, R.S., Correa Barbosa, A.V., Palheta de Sousa, D.J., Silva Teixeira, J.S., de Santana Botelho, A., 2019. Effect of cadmium on young plants of *Virola surinamensis*. AoB Plants. https://doi.org/10.1093/aobpla/plz022.

[6] Baritz, R., Amelung, W., Antoni, V., Boardman, J., Horn, R., Prokop, G., Römbke, J., Romkens, P., Steinhoff-Knopp, B., Swartjes, F., Trombetti, M., De Vries, W., 2021. Soil monitoring in Europe: indicators and thresholds for soil quality assessments. Version 24 Sept. 2021 for REVIEW 1–148.

[7] Ben-Shem, A., Frolow, F., Nelson, N., 2003. Crystal structure of plant photosystem I. Nature 426, 630–635. https://doi.org/10.1038/nature02200.

[9] Clemens, S., Aarts, M.G.M., Thomine, S., Verbruggen, N., 2013. Plant science: the key to preventing slow cadmium poisoning. Trends Plant Sci 18, 92–99. https://doi.org/10.1016/j.tplants.2012.08.003.

[10] Cui, X., Mao, P., Sun, S., Huang, R., Fan, Y., Li, Yongxing, Li, Yingwen, Zhuang, P., Li, Z., 2021. Phytoremediation of cadmium contaminated soils by *Amaranthus hypochondriacus* L.: The effects of soil properties highlighting cation exchange capacity. Chemosphere 283, 131067. https://doi.org/10.1016/j.chemosphere.2021.131067.

[11] Diarra, I., Kotra, K.K., Prasad, S., 2021. Application of phytoremediation for heavy metal contaminated sites in the South Pacific: strategies, current challenges and future prospects. Appl Spectrosc Rev 1–23. https://doi.org/10.1080/05704928.2021.1904410.

[12] Dikšaitytė, A., Viršilė, A., Žaltauskaitė, J., Januškaitienė, I., Juozapaitienė, G., 2019. Growth and photosynthetic responses in *Brassica napus* differ during stress and recovery periods when exposed to combined heat, drought and elevated CO_2. Plant Physiol Biochem 142, 59–72. https://doi.org/10.1016/j.plaphy.2019.06.026.

[13] Dikšaitytė, A., Viršilė, A., Žaltauskaitė, J., Januškaitienė, I., Praspaliauskas, M., Pedišius, N., 2020. Do plants respond and recover from a combination of drought and heatwave in the same manner under adequate and deprived soil nutrient conditions? Plant Sci 291, 110333. https://doi.org/10.1016/j.plantsci.2019.110333.

[14] Dobrikova, A.G., Apostolova, E.L., Hanć, A., Yotsova, E., Borisova, P., Sperdouli, I., Adamakis, I.-D.S., Moustakas, M., 2021. Cadmium toxicity in *Salvia sclarea* L.: An integrative response of element uptake, oxidative stress markers, leaf structure and photosynthesis. Ecotoxicol Environ Saf 209, 111851. https://doi.org/10.1016/j.ecoenv.2020.111851.

[15] Droppa, M., Horváth, G., 1990. The role of copper in photosynthesis. CRC. Crit. Rev. Plant Sci. https://doi.org/10.1080/07352689009382284.

[16] Droppa, M., Terry, N., Horvath, G., 1984. Effects of Cu deficiency on photosynthetic electron transport. Proc Natl Acad Sci. https://doi.org/10.1073/pnas.81.8.2369.

[17] Duan, H., Wu, J., Huang, G., Zhou, S., Liu, W., Liao, Y., Yang, X., Xiao, Z., Fan, H., 2016. Individual and interactive effects of drought and heat on leaf physiology of seedlings in an economically important crop. AoB Plants 9 plw090. https://doi.org/10.1093/aobpla/plw090.

[18] Dutta, A., Patra, A., Singh Jatav, H., Singh Jatav, S., Kumar Singh, S., Sathyanarayana, E., Verma, S., Singh, P., 2021. Toxicity of cadmium in soil-plant-human continuum and its bioremediation techniques. In: Toxicity of cadmium in soil-plant-human continuum and its bioremediation techniques. Soil contamination – threats and sustainable solutions. https://doi.org/10.5772/intechopen.94307.

[19] Egnér, H., Riehm, H., Domingo, W.R., 1960. Untersuchungen über die chemische bodenanalyse als grundlage für die beurteilung des nährstoffzustandes der böden. II. Chemische extraktionsmethoden zur phosphor- und kaliumbestimmung. K Lantbr Ann 26, 199–215.

[20] Elferjani, R., Soolanayakanahally, R., 2018. Canola responses to drought, heat, and combined stress: shared and specific effects on carbon assimilation, seed yield, and oil composition. Front Plant Sci 9, 1–17. https://doi.org/10.3389/fpls.2018.01224.

[21] Esmaeilizadeh, M., Malekzadeh Shamsabad, M.R., Roosta, H.R., Dąbrowski, P., Rapacz, M., Zieliński, A., Wróbel, J., Kalaji, H.M., 2021. Manipulation of light spectrum can improve the performance of photosynthetic apparatus of strawberry plants growing under salt and alkalinity stress. PLoS One 16, e0261585. https://doi.org/10.1371/journal.pone.0261585.

[22] Fahad, S., Bajwa, A.A., Nazir, U., Anjum, S.A., Farooq, A., Zohaib, A., Sadia, S., Nasim, W., Adkins, S., Saud, S., Ihsan, M.Z., Alharby, H., Wu, C., Wang, D., Huang, J., 2017. Crop production under drought and heat stress: plant responses and management options. Front Plant Sci 8, 1–16. https://doi.org/10.3389/fpls.2017.01147.

[23] Faller, P., Kienzler, K., Krieger-Liszkay, A., 2005. Mechanism of Cd^{2+} toxicity: Cd^{2+} inhibits photoactivation of Photosystem II by competitive binding to the essential Ca^{2+} site. Biochim Biophys Acta - Bioenerg 1706, 158–164. https://doi.org/10.1016/j.bbabio.2004.10.005.

[24] Feszterová, M., Porubcová, L., Tirpáková, A., 2021. The monitoring of selected heavy metals content and bioavailability in the soil-plant system and its impact on sustainability in agribusiness food chains. Sustainability 13, 7021. https://doi.org/10.3390/su13137021.

[25] Franić, M., Galić, V., Lončarić, Z., Šimić, D., 2020. Genotypic variability of photosynthetic parameters in maize ear-leaves at different cadmium levels in soil. Agronomy. https://doi.org/10.3390/agronomy10070986.

[26] Fukuyama, K., Hase, T., Matsumoto, S., Tsukihara, T., Katsube, Y., Tanaka, N., Kakudo, M., Wada, K., Matsubara, H., 1980. Structure of *S. platensis* [2Fe-2S] ferredoxin and evolution of chloroplast-type ferredoxins. Nature. https://doi.org/10.1038/286522a0.

[27] Ge, L.-Q., Cang, L., Liu, H., Zhou, D.-M., 2016. Effects of warming on uptake and translocation of cadmium (Cd) and copper (Cu) in a contaminated soil-rice system

under Free Air Temperature Increase (FATI). Chemosphere 155, 1–8. https://doi.org/10.1016/j.chemosphere.2016.04.032.

[28] Gillet, S., Decottignies, P., Chardonnet, S., Le Maréchal, P., 2006. Cadmium response and redoxin targets in Chlamydomonas reinhardtii: a proteomic approach. Photosynth Res 89, 201–211. https://doi.org/10.1007/s11120-006-9108-2.

[29] Global and European temperatures. 2022. Retrieved December 30, 2022, from https://www.eea.europa.eu/ims/global-and-european-temperatures.

[30] Goltsev, V.N., Kalaji, H.M., Paunov, M., Bąba, W., Horaczek, T., Mojski, J., Kociel, H., Allakhverdiev, S.I., 2016. Variable chlorophyll fluorescence and its use for assessing physiological condition of plant photosynthetic apparatus. Russ J Plant Physiol. https://doi.org/10.1134/S1021443716050058.

[31] Gupta, R., 2020. The oxygen-evolving complex: a super catalyst for life on earth, in response to abiotic stresses. Plant Signal Behav 15, 1824721. https://doi.org/10.1080/15592324.2020.1824721.

[32] Haider, F.U., Liqun, C., Coulter, J.A., Cheema, S.A., Wu, J., Zhang, R., Wenjun, M., Farooq, M., 2021. Cadmium toxicity in plants: impacts and remediation strategies. Ecotoxicol Environ Saf 211, 111887. https://doi.org/10.1016/j.ecoenv.2020.111887.

[33] Hauptvogl, M., Kotrla, M., Prčík, M., Pauková, Ž., Kováčik, M., Lošák, T., 2019. Phytoremediation potential of fast-growing energy plants: challenges and perspectives – a review. Pol J Environ Stud 29, 505–516. https://doi.org/10.15244/pjoes/101621.

[34] He, S., Yang, X., He, Z., Baligar, V.C., 2017. Morphological and physiological responses of plants to cadmium toxicity: a review. Pedosphere. https://doi.org/10.1016/S1002-0160(17)60339-4.

[35] Hédiji, H., Djebali, W., Belkadhi, A., Cabasson, C., Moing, A., Rolin, D., Brouquisse, R., Gallusci, P., Chaïbi, W., 2015. Impact of long-term cadmium exposure on mineral content of *Solanum lycopersicum* plants: consequences on fruit production. South Afr J Bot. https://doi.org/10.1016/j.sajb.2015.01.010.

[36] Huang, R., Dong, M., Mao, P., Zhuang, P., Paz-Ferreiro, J., Li, Yongxing, Li, Yingwen, Hu, X., Netherway, P., Li, Z., 2020. Evaluation of phytoremediation potential of five Cd (hyper)accumulators in two Cd contaminated soils. Sci Total Environ 721, 137581. https://doi.org/10.1016/j.scitotenv.2020.137581.

[37] Hurt, E., Hauska, G., 2005. A cytochrome f/b6 complex of five polypeptides with plastoquinol-plastocyanin-oxidoreductase activity from spinach chloroplasts. Eur J Biochem 117, 591–599. https://doi.org/10.1111/j.1432-1033.1981.tb06379.x.

[38] Hussain, C.M., Keçili, R., 2020. Environmental pollution and environmental analysis. In: Modern environmental analysis techniques for pollutants. Elsevier, pp. 1–36. https://doi.org/10.1016/B978-0-12-816934-6.00001-1.

[39] IPCC, 2021. IPCC: Climate Change 2021. The Physical Science Basis (Summary for Policymakers). Cambridge Univ. Press. Press,.

[40] Janeeshma, E., Kalaji, H.M., Puthur, J.T., 2021. Differential responses in the photosynthetic efficiency of *Oryza sativa* and *Zea mays* on exposure to Cd and Zn toxicity. Acta Physiol Plant 43, 12. https://doi.org/10.1007/s11738-020-03178-x.

[41] Jia, Y., Tang, S., Wang, R., Ju, X., Ding, Y., Tu, S., Smith, D.L., 2010. Effects of elevated CO_2 on growth, photosynthesis, elemental composition, antioxidant level, and phytochelatin concentration in *Lolium mutiforum* and *Lolium perenne* under Cd stress. J Hazard Mater 180, 384–394. https://doi.org/10.1016/j.jhazmat.2010.04.043.

[43] Juozapaitienė, G., Dikšaitytė, A., Sujetovienė, G., Aleinikovienė, J.ū., Juknys, R., 2019. Aboveground and below-ground carbon allocation of summer rape under elevated CO_2 and air temperature. Agric Food Sci 28. https://doi.org/10.23986/afsci.70460.

[44] Kalaji, H.M., Račková, L., Paganová, V., Swoczyna, T., Rusinowski, S., Sitko, K., 2018. Can chlorophyll-a fluorescence parameters be used as bio-indicators to distinguish between drought and salinity stress in *Tilia cordata* Mill? Environ Exp Bot. https://doi.org/10.1016/j.envexpbot.2017.11.001.

[45] Khalef, R.N., Hassan, A.I., Saleh, H.M., 2022. Heavy metal's environmental impact, in: Environmental impact and remediation of heavy metals. https://doi.org/10.5772/intechopen.103907.

[46] Kochare, T., Tamir, B., 2015. Assessment of dairy feeds for heavy metals. Am Sci Res J Eng 11 (1), 20–31.

[47] Kroh, G.E., Pilon, M., 2020. Regulation of iron homeostasis and use in chloroplasts. Int J Mol Sci 21, 3395. https://doi.org/10.3390/ijms21093395.

[48] Krupa, Z., Siedlecka, A., Skórzynska-Polit, E., Maksymiec, W., 2002. Heavy metal interactions with plant nutrients. In: Physiology and biochemistry of metal toxicity and tolerance in plants. Springer, Netherlands, Dordrecht, pp. 287–301. https://doi.org/10.1007/978-94-017-2660-3_11.

[49] Kubier, A., Wilkin, R.T., Pichler, T., 2019. Cadmium in soils and groundwater: a review. Appl Geochem. https://doi.org/10.1016/j.apgeochem.2019.104388.

[50] Kumar, D., Singh, H., Raj, S., Soni, V., 2020. Chlorophyll *a* fluorescence kinetics of mung bean (*Vigna radiata* L.) grown under artificial continuous light. Biochem Biophys Rep. https://doi.org/10.1016/j.bbrep.2020.100813.

[51] Lamaoui, M., Jemo, M., Datla, R., Bekkaoui, F., 2018. Heat and drought stresses in crops and approaches for their mitigation. Front Chem 6, 1–14. https://doi.org/10.3389/fchem.2018.00026.

[52] Li, L.-Z., Tu, C., Wu, L.-H., Peijnenburg, W.J.G.M., Ebbs, S., Luo, Y.-M., 2017. Pathways of root uptake and membrane transport of Cd^{2+} in the zinc/cadmium hyperaccumulating plant *Sedum plumbizincicola*. Environ Toxicol Chem 36, 1038–1046. https://doi.org/10.1002/etc.3625.

[53] Li, X., Li, Yilun, Zhu, X., Gui, X., Ma, C., Peng, W., Li, Yongsheng, Zhang, Y., Huang, W., Hua, D., Jia, S., Wu, M., 2022. Evaluation of the cadmium phytoextraction potential of tobacco (*Nicotiana tabacum*) and rhizosphere micro-characteristics under different cadmium levels. Chemosphere 286, 131714. https://doi.org/10.1016/j.chemosphere.2021.131714.

[54] Li, Y., Zhang, Q., Wang, R., Gou, X., Wang, H., Wang, S., 2012. Temperature changes the dynamics of trace element accumulation in *Solanum tuberosum* L. Clim Change 112, 655–672. https://doi.org/10.1007/s10584-011-0251-1.

[55] Li, Z., Tang, S., Deng, X., Wang, R., Song, Z., 2010. Contrasting effects of elevated CO_2 on Cu and Cd uptake by different rice varieties grown on contaminated soils with two levels of metals: implication for phytoextraction and food safety. J Hazard Mater 177, 352–361. https://doi.org/10.1016/j.jhazmat.2009.12.039.

[56] Lindsey, R., 2022. Climate change: atmospheric carbon dioxide. NOAA Clim 1–5, 2022.

[57] Liu, C., Yu, R., Shi, G., 2017. Effects of drought on the accumulation and redistribution of cadmium in peanuts at different developmental stages. Arch Agron Soil Sci 63, 1049–1057. https://doi.org/10.1080/03650340.2016.1271120.

[58] Liu, Y., Liu, K., Li, Y., Yang, W., Wu, F., Zhu, P., Zhang, J., Chen, L., Gao, S., Zhang, L., 2016. Cadmium contamination of soil and crops is affected by intercropping and rotation systems in the lower reaches of the Minjiang River in south-western China. Environ Geochem Health 38, 811–820. https://doi.org/10.1007/s10653-015-9762-4.

[59] Loix, C., Huybrechts, M., Vangronsveld, J., Gielen, M., Keunen, E., Cuypers, A., 2017. Reciprocal interactions between cadmium-induced cell wall responses and oxidative stress in plants. Front Plant Sci. https://doi.org/10.3389/fpls.2017.01867.

[60] Mathur, S., Kalaji, H.M., Jajoo, A., 2016. Investigation of deleterious effects of chromium phytotoxicity and photosynthesis in wheat plant. Photosynthetica 54 (2), 185–192. https://doi.org/10.1007/s11099-016-0198-6.

[61] Merchant, S., Sawaya, M.R., 2005. The light reactions: A guide to recent acquisitions for the picture gallery. Plant Cell 17, 648–663. https://doi.org/10.1105/tpc.105.030676.

[62] Mourato, M., Pinto, F., Moreira, I., Sales, J., Leitão, I., Martins, L.L., 2018. The effect of Cd stress in mineral nutrient uptake in plants. Cadmium Toxic Toler Plant: Physiol Remediat. https://doi.org/10.1016/B978-0-12-814864-8.00013-9.

[63] Naciri, R., Lahrir, M., Benadis, C., Chtouki, M., Oukarroum, A., 2021. Interactive effect of potassium and cadmium on growth, root morphology and chlorophyll a fluorescence in tomato plant. Sci Rep 11, 5384. https://doi.org/10.1038/s41598-021-84990-4.

[64] Pagliano, C., Raviolo, M., Dalla Vecchia, F., Gabbrielli, R., Gonnelli, C., Rascio, N., Barbato, R., La Rocca, N., 2006. Evidence for PSII donor-side damage and photoinhibition induced by cadmium treatment on rice (*Oryza sativa* L.). J Photochem Photobiol B 84, 70–78. https://doi.org/10.1016/j.jphotobiol.2006.01.012.

[65] Parmar, P., Kumari, N., Sharma, V., 2013. Structural and functional alterations in photosynthetic apparatus of plants under cadmium stress. Bot Stud. https://doi.org/10.1186/1999-3110-54-45.

[66] Paunov, M., Koleva, L., Vassilev, A., Vangronsveld, J., Goltsev, V., 2018. Effects of different metals on photosynthesis: cadmium and zinc affect chlorophyll fluorescence in durum wheat. Int J Mol Sci 19, 787. https://doi.org/10.3390/ijms19030787.

[67] Perfus-Barbeoch, L., Leonhardt, N., Vavasseur, A., Forestier, C., 2002. Heavy metal toxicity: cadmium permeates through calcium channels and disturbs the plant water status. Plant J 32, 539–548. https://doi.org/10.1046/j.1365-313X.2002.01442.x.

[68] Pietrini, F., Zacchini, M., Iori, V., Pietrosanti, L., Ferretti, M., Massacci, A., 2009. Spatial distribution of cadmium in leaves and its impact on photosynthesis: examples of different strategies in willow and poplar clones. Plant Biol 12, 355–363. https://doi.org/10.1111/j.1438-8677.2009.00258.x.

[69] Pourghasemian, N., Ehsanzadeh, P., Greger, M., 2013. Genotypic variation in safflower (*Carthamus* spp.) cadmium accumulation and tolerance affected by temperature and cadmium levels. Environ Exp Bot. https://doi.org/10.1016/j.envexpbot.2012.12.003.

[70] Rahim, H.U., Akbar, W.A., Alatalo, J.M., 2022. A comprehensive literature review on cadmium (Cd) status in the soil environment and its immobilization by biochar-based materials. Agronomy 12, 877. https://doi.org/10.3390/agronomy12040877.

[71] Rajkumar, M., Prasad, M.N.V., Swaminathan, S., Freitas, H., 2013. Climate change driven plant–metal–microbe interactions. Environ Int 53, 74–86. https://doi.org/10.1016/j.envint.2012.12.009.

[72] Rawat, J., Pandey, N., Saxena, J., 2022. Role of potassium in plant photosynthesis, transport, growth and yield. Role Potassium abiotic Stress. https://doi.org/10.1007/978-981-16-4461-0_1.

[73] Rivero, R.M., Mittler, R., Blumwald, E., Zandalinas, S.I., 2021. Developing climate-resilient crops: improving plant tolerance to stress combination. Plant J. https://doi.org/10.1111/tpj.15483.

[74] Ruggiero, A., Punzo, P., Landi, S., Costa, A., Van Oosten, M., Grillo, S., 2017. Improving plant water use efficiency through molecular genetics. Horticulturae 3, 31. https://doi.org/10.3390/horticulturae3020031.

[75] Sadeghzadeh, B., 2013. A review of zinc nutrition and plant breeding. J Soil Sci Plant Nutr. https://doi.org/10.4067/S0718-95162013005000072.

[76] Samborska, I.A., Kalaji, H.M., Sieczko, L., Borucki, W., Mazur, R., Kouzmanova, M., Goltsev, V., 2019. Can just one-second measurement of chlorophyll a fluorescence be used to predict sulphur deficiency in radish (*Raphanus sativus* L. sativus) plants? Curr Plant Biol 19, 100096. https://doi.org/10.1016/j.cpb.2018.12.002.

[77] Sarwar, N., Saifullah, Malhi, S.S., Zia, M.H., Naeem, A., Bibi, S., Farid, G., 2010. Role of mineral nutrition in minimizing cadmium accumulation by plants. J Sci Food Agric 90, 925–937. https://doi.org/10.1002/jsfa.3916.

[78] Schansker, G., Tóth, S.Z., Strasser, R.J., 2005. Methylviologen and dibromothymoquinone treatments of pea leaves reveal the role of photosystem I in the Chl *a* fluorescence rise OJIP. Biochim Biophys Acta - Bioenerg 1706, 250–261. https://doi.org/10.1016/j.bbabio.2004.11.006.

[79] Shaari, N.E.M., Tajudin, M.T.F.M., Khandaker, M.M., Majrashi, A., Alenazi, M.M., Abdullahi, U.A., Mohd, K.S., 2022. Cadmium toxicity symptoms and uptake mechanism in plants: a review. Braz J Biol 84, e252143. https://doi.org/10.1590/1519-6984.252143.

[80] Shahbaz, M., Ravet, K., Peers, G., Pilon, M., 2015. Prioritization of copper for the use in photosynthetic electron transport in developing leaves of hybrid poplar. Front Plant Sci. https://doi.org/10.3389/fpls.2015.00407.

[81] Shi, G., Xia, S., Ye, J., Huang, Y., Liu, C., Zhang, Z., 2015. PEG-simulated drought stress decreases cadmium accumulation in castor bean by altering root morphology. Environ Exp Bot. https://doi.org/10.1016/j.envexpbot.2014.11.008.

[82] Silva Cunha, L.F., Oliveira, V.P., Nascimento, A.W.S., Silva, B.R.S., Batista, B.L., Alsahli, A.A., Lobato, A.K., da, S., 2020. Leaf application of 24–epibrassinolide mitigates cadmium toxicity in young *Eucalyptus urophylla* plants by modulating leaf anatomy and gas exchange (ppl.). Physiol Plant 13182. https://doi.org/10.1111/ppl.13182.

[83] Song, X., Yue, X., Chen, W., Jiang, H., Han, Y., Li, X., 2019. Detection of cadmium risk to the photosynthetic performance of *Hybrid pennisetum*. Front Plant Sci. https://doi.org/10.3389/fpls.2019.00798.

[84] World Meteorological Organization (WMO). 2022. State of the Climate in Europe2021(WMO-No. 1304). Geneva.

[85] Strasser, B.J., 1997. Donor side capacity of Photosystem II probed by chlorophyll *a* fluorescence transients. Photosynth Res. https://doi.org/10.1023/A:1005896029778.

[86] Stirbet, A., Govindjee, 2011. On the relation between the Kautsky effect (chlorophyll *a* fluorescence induction) and photosystem II: basics and applications of the OJIP fluorescence transient. J Photochem Photobiol B Biol. https://doi.org/10.1016/j.jphotobiol.2010.12.010.

[87] Stirbet, A., Lazár, D., Kromdijk, J., Govindjee, 2018. Chlorophyll *a* fluorescence induction: can just a one-second measurement be used to quantify abiotic stress responses? Photosynthetica. https://doi.org/10.1007/s11099-018-0770-3.

[88] Strasser, R.J., Srivastava, A., Tsimilli-Michael, M., 2000. The fluorescence transient as a tool to characterize and screen photosynthetic samples. Probing Photosynth Mech Regul Adapt.

[89] Strasser, R.J., Tsimilli-Michael, M., Qiang, S., Goltsev, V., 2010. Simultaneous in vivo recording of prompt and delayed fluorescence and 820 nm reflection changes during drying and after rehydration of the resurrection plant *Haberlea rhodopensis*. Biochim Biophys Acta - Bioenerg 1797, 122. https://doi.org/10.1016/j.bbabio.2010.04.365.

[90] Suman, J., Uhlik, O., Viktorova, J., Macek, T., 2018. Phytoextraction of heavy metals: a promising tool for clean-up of polluted environment? Front Plant Sci. https://doi.org/10.3389/fpls.2018.01476.

[91] Szopiński, M., Sitko, K., Gieroń, Ż., Rusinowski, S., Corso, M., Hermans, C., Verbruggen, N., Małkowski, E., 2019. Toxic effects of cd and zn on the photosynthetic apparatus of the *Arabidopsis halleri* and *Arabidopsis arenosa* pseudo-metallophytes. Front Plant Sci. https://doi.org/10.3389/fpls.2019.00748.

[92] Tebaldi, C., Debeire, K., Eyring, V., Fischer, E., Fyfe, J., Friedlingstein, P., Knutti, R., Lowe, J., O'Neill, B., Sanderson, B., van Vuuren, D., Riahi, K., Meinshausen, M., Nicholls, Z., Tokarska, K.B., Hurtt, G., Kriegler, E., Lamarque, J.-F., Meehl, G., Moss, R., Bauer, S.E., Boucher, O., Brovkin, V., Byun, Y.-H., Dix, M., Gualdi, S., Guo, H., John, J.G., Kharin, S., Kim, Y., Koshiro, T., Ma, L., Olivié, D., Panickal, S., Qiao, F., Rong, X., Rosenbloom, N., Schupfner, M., Séférian, R., Sellar, A., Semmler, T., Shi, X., Song, Z., Steger, C., Stouffer, R., Swart, N., Tachiiri, K., Tang, Q., Tatebe, H., Voldoire, A., Volodin, E., Wyser, K., Xin, X., Yang, S., Yu, Y., Ziehn, T., 2021. Climate model projections from the Scenario Model Intercomparison Project (ScenarioMIP) of CMIP6. Earth Syst Dyn 12, 253–293. https://doi.org/10.5194/esd-12-253-2021.

[93] Tikhonov, A.N., 2014. The cytochrome b6f complex at the crossroad of photosynthetic electron transport pathways. Plant Physiol Biochem 81, 163–183. https://doi.org/10.1016/j.plaphy.2013.12.011.

[94] Tripathi, S., Arora, N., Pruthi, V., Poluri, K.M., 2021. Elucidating the bioremediation mechanism of *Scenedesmus* sp. IITRIND2 under cadmium stress. Chemosphere 283, 131196. https://doi.org/10.1016/j.chemosphere.2021.131196.

[95] Van Ginneken, L., Meers, E., Guisson, R., Ruttens, A., Elst, K., Tack, F.M.G., Vangronsveld, J., Diels, L., Dejonghe, W., 2007. Phytoremediation for heavy metal-contaminated soils combined with bioenergy production. J Environ Eng Landsc Manag. https://doi.org/10.1080/16486897.2007.9636935.

[96] Wang, L., Rinklebe, J., Tack, F.M.G., Hou, D., 2021. A review of green remediation strategies for heavy metal contaminated soil. Soil Use Manag 37, 936–963. https://doi.org/10.1111/sum.12717.

[97] Wang, X., Zheng, M., Liu, H., Zhang, L., Chen, F., Zhang, W., Fan, S., Peng, M., Hu, M., Wang, H., Zhang, J., Hua, W., 2020. Fine-mapping and transcriptome analysis of a candidate gene controlling plant height in *Brassica napus* L. Biotechnol Biofuels 13, 42. https://doi.org/10.1186/s13068-020-01687-y.

[98] Xia, S., Wang, X., Su, G., Shi, G., 2015. Effects of drought on cadmium accumulation in peanuts grown in a contaminated calcareous soil. Environ Sci Pollut Res 22, 18707–18717. https://doi.org/10.1007/s11356-015-5063-9.

[99] Xu, S.S., Lin, S.Z., Lai, Z.X., 2015. Cadmium impairs iron homeostasis in *Arabidopsis thaliana* by increasing the polysaccharide contents and the iron-binding capacity of root cell walls. Plant Soil 392, 71–85. https://doi.org/10.1007/s11104-015-2443-3.

[100] Xue, S., Shi, L., Wu, C., Wu, H., Qin, Y., Pan, W., Hartley, W., Cui, M., 2017. Cadmium, lead, and arsenic contamination in paddy soils of a mining area and their exposure effects on human HEPG2 and keratinocyte cell-lines. Environ Res 156, 23–30. https://doi.org/10.1016/j.envres.2017.03.014.

[101] Yan, A., Wang, Y., Tan, S.N., Mohd Yusof, M.L., Ghosh, S., Chen, Z., 2020. Phytoremediation: a promising approach for revegetation of heavy metal-polluted land. Front Plant Sci. https://doi.org/10.3389/fpls.2020.00359.

[102] Yotsova, E., Dobrikova, A., Stefanov, M., Misheva, S., Bardáčová, M., Matušíková, I., Žideková, L., Blehová, A., Apostolova, E., 2020. Effects of cadmium on two wheat cultivars depending on different nitrogen supply. Plant Physiol Biochem 155, 789–799. https://doi.org/10.1016/j.plaphy.2020.06.042.

[103] Yusuf, M.A., Kumar, D., Rajwanshi, R., Strasser, R.J., Tsimilli-Michael, M., Govindjee, Sarin, N.B., 2010. Overexpression of γ-tocopherol methyl transferase gene in transgenic *Brassica juncea* plants alleviates abiotic stress: Physiological and chlorophyll *a* fluorescence measurements. Biochim Biophys Acta - Bioenerg 1797, 1428–1438. https://doi.org/10.1016/j.bbabio.2010.02.002.

[104] Zandalinas, S.I., Mittler, R., Balfagón, D., Arbona, V., Gómez-Cadenas, A., 2018. Plant adaptations to the combination of drought and high temperatures. Physiol Plant 162, 2–12. https://doi.org/10.1111/ppl.12540.

[105] Zhang, C., Jia, X., Zhao, Y., Wang, L., Cao, K., Zhang, N., Gao, Y., Wang, Z., 2021. The combined effects of elevated atmospheric CO_2 and cadmium exposure on flavonoids in the leaves of *Robinia pseudoacacia* L. seedlings. Ecotoxicol Environ Saf 210, 111878. https://doi.org/10.1016/j.ecoenv.2020.111878.

[106] Zulfiqar, U., Jiang, W., Xiukang, W., Hussain, S., Ahmad, M., Maqsood, M.F., Ali, N., Ishfaq, M., Kaleem, M., Haider, F.U., Farooq, N., Naveed, M., Kucerik, J., Brtnicky, M., Mustafa, A., 2022. Cadmium phytotoxicity, tolerance, and advanced remediation approaches in agricultural soils; a comprehensive review. Front Plant Sci 13, 1–33. https://doi.org/10.3389/fpls.2022.773815.